LOFT-TR-103
for U.S. Nuclear Regulatory Commission

QUICK LOOK REPORT ON LOFT NUCLEAR EXPERIMENT L2-2

DOYLE L. BATT

December 1978

EG&G Idaho, Inc.

IDAHO NATIONAL ENGINEERING LABORATORY

DEPARTMENT OF ENERGY

IDAHO OPERATIONS OFFICE UNDER CONTRACT EY-76-C-07-1570

"The NRC will make available data tapes and operational computer codes on research programs dealing with postulated loss-of-coolant accidents in light water reactors. Persons requesting this information must reimburse the NRC contractors for their expenses in preparing copies of the data tapes and the operational computer codes. Requests should be submitted to the Research Applications Branch, Office of Nuclear Regulatory Research, Nuclear Regulatory Commission, Washington, D.C. 20555."

QUICK LOOK REPORT ON LOFT NUCLEAR EXPERIMENT L2-2

Approved:

S. A. Naff for L. P. Leach

L.P. Leach, Manager

LOFT Experimental Program Division

W. A. Spencer

for N.C. Kaufman, Director

LOFT

The information contained in this summary report is preliminary and incomplete. Selected pertinent data are presented in order to draw preliminary conclusions and to expedite the reporting of research results.

LOFT-TR-103

QUICK LOOK REPORT ON LOFT NUCLEAR EXPERIMENT L2-2

Doyle L. Batt

EG&G Idaho, Inc.
Idaho Falls, Idaho 83401

Published December 1978

PREPARED FOR THE
U.S. NUCLEAR REGULATORY COMMISSION
AND THE U.S. DEPARTMENT OF ENERGY
IDAHO OPERATIONS OFFICE
UNDER CONTRACT NO. EY-76-C-07-1570
NRC FIN NO. A6048

SUMMARY

This report presents a preliminary evaluation and summary of the results of the first LOFT nuclear loss-of-coolant experiment (LOCE), LOCE L2-2, which was successfully conducted on December 9, 1978. LOCE L2-2 is the first experiment in the power ascension series as defined in Volume I of the Experiment Operating Specification. LOCE L2-2 simulated a complete double-ended offset shear break of a large pressurized water reactor inlet pipe. Selected data are presented in this report to confirm that the objectives of LOCE L2-2, as defined in Volume 2 of the Experiment Operating Specification, were met. The experiment was successful in achieving all objectives.

At the time of break initiation, the nuclear core was operating at a steady state maximum linear heat generation rate of 26.38 kW/m. Other significant initial conditions for LOCE L2-2 were: system pressure, 15.64 $\pm$ 0.2 MPa; core outlet temperature, 580.4 $\pm$ 3.0 K; and intact loop flow rate, 194.2 $\pm$ 6.3 kg/s. Scaled quantities of high pressure, low pressure, and accumulator emergency core coolant were injected during the LOCE. The primary coolant pumps were operated at constant speed throughout the experiment.

The experiment proceeded as planned, starting with a rapid (100 ms) drop to hot fluid saturation pressure after simultaneous opening of the quick-opening valves in 18 ms. The hot pins of the core entered departure from nucleate boiling at about 1.6 s ($\overline{X}$ = 1.635, s = 0.276 for the center fuel module) after rupture initiation and reached a peak cladding temperature of 789 K at 5.8 s after rupture. The emergency core coolant started flow from the high-pressure system at 12 s, the accumulator system at 18 s, and the low-pressure system at 29 s after rupture. The latest quench occurred at 44 s after rupture.

The instrumentation and data acquisition system performed well. It is estimated that 872 (95%) of the 922 instruments (includes discrete

event measurements) recorded operated satisfactorily. The plant protection system (PPS) was operational and performed within the experimental band. The control rods were fully inserted within 1.725 s after the initiation of rupture.

The RELAP4/MOD6 pretest prediction of thermal-hydraulic response in the primary coolant system appears to compare reasonably well with LOCE L2-2 data. The fuel clad temperature response predicted by RELAP4/MOD6 and FRAP-T4 did not agree with LOCE L2-2 data except in regions near the periphery of the core and resulted in overprediction of peak clad temperature by approximately 200 K. TRAC predicted peak clad temperature was higher than LOCE L2-2 by approximately 135 K. All codes predicted final quench to occur later than was measured by as much as 50 s.

LOFT LOCE L2-2, the first experiment in the power ascension series, provided experimental data on thermal-hydraulic behavior, nuclear core response, and the behavior of emergency core cooling systems during a loss-of-coolant accident in a pressurized water nuclear reactor. The intensive analysis of the results of LOCE L2-2 currently underway will result in additional understanding of loss-of-coolant accidents and together with results from other Nuclear Regulatory Commission experimental programs will provide the basis required for development and assessment of analytical models for licensing commercial pressurized water reactors.

CONTENTS

FIGURES

TABLES

QUICK LOOK REPORT ON LOFT NUCLEAR EXPERIMENT L2-2

1. INTRODUCTION

Loss-of-Coolant Experiment (LOCE) L2-2, the first in the power ascension series of nuclear LOCEs (Test Series L2) scheduled for performance in the LOFT facility, was successfully completed December 9, 1978. Test Series L2 is the first series of nuclear LOCEs and was designed to provide large scale integrated plant data on thermal-hydraulic and fuel behavior. The general requirements for the LOFT Test Series L2 are specified in Reference 1.

The specific objectives for LOCE L2-2, as stated in Reference 2, are as follows, they include objectives from LOCE L2-1, which was deleted from Test Series L2:

(1) Objective 1: Provide a test in which the hottest fuel pins are predicted to encounter departure from nucleate boiling (DNB) and not immediately reenter the nucleate boiling heat transfer regime to allow assessment of fuel rod-to-coolant heat transfer in the post-critical heat flux (CHF) regime.

(2) Objective 2: Check out experimental and process instrumentation pertaining to nuclear LOCE performance.

(3) Objective 3: Determine overall performance of the LOFT facility in nuclear LOCE operation and locate any equipment/procedures that require upgrading prior to nuclear LOCE performance at higher power levels.

(4) Objective 4: Provide data to evaluate LOFT emergency core cooling system (ECCS) scaling techniques in the blowdown of a system operating at power.

(5) Objective 5: Determine LOFT fuel rod temperature response in a 26.2 kW/m maximum linear heat generation rate (MLHGR) double-ended cold leg break LOCE.

(6) Objective 6: Determine blowdown thermal-hydraulic response at 67% nominal hot-leg-to-cold-leg temperature difference of 23.9 K.

(7) Objective 7: Determine if any clad perforation occurs in a 26.2 kW/m MLHGR double-ended cold leg break LOCE.

(8) Objective 8: Provide integral nuclear system code verification data on a low-to-intermediate power double-ended cold leg break.

(9) Objective 9: Determine LOFT reflood characteristics at 26.2 kW/m MLHGR initial condition.

This report presents a preliminary examination of the plant performance (Section 2) and a summary of the results from LOFT LOCE L2-2 (Section 3). Section 4 presents conclusions reached from this examination of preliminary results. Data are presented in Section 5 to allow a preliminary evaluation of LOCE L2-2 in satisfying the test objectives. The data plots presented include comparisons of LOCE L2-2 data with (a) Semiscale Test S-06-2[3], which is the counterpart to LOCE L2-2; (b) LOCE L2-2 pretest prediction[4] using the RELAP4/MOD6[5] and FRAP-T4[6] computer codes; and (c) LOCE L2-2 pretest prediction made by Los Alamos Scientific Laboratory[7] using the TRAC[8] computer code.

LOCE L2-2 simulated a 200% (100% break area in each leg of the LOFT broken loop) double-ended offset shear in the cold leg of a four-loop large pressurized water reactor (PWR). To help in understanding the results from LOCE L2-2, a drawing of the LOFT system geometry is shown in Figure 1 and a representation of the core configuration illustrating the instrumentation is shown in Figure 2. Additional details of the core and fuel modules are given in Reference 9.

A complete list of the LOFT instrumentation and data acquisition requirements for LOCE L2-2 is given in Reference 2. LOFT radiation hardened densitometers are new instruments installed for LOCE L2-2 and are illustrated in a schematic drawing on Figure 3. To aid in interpreting the identification of the system instrumentation, the terminology used for transducer identification is given in Table I.

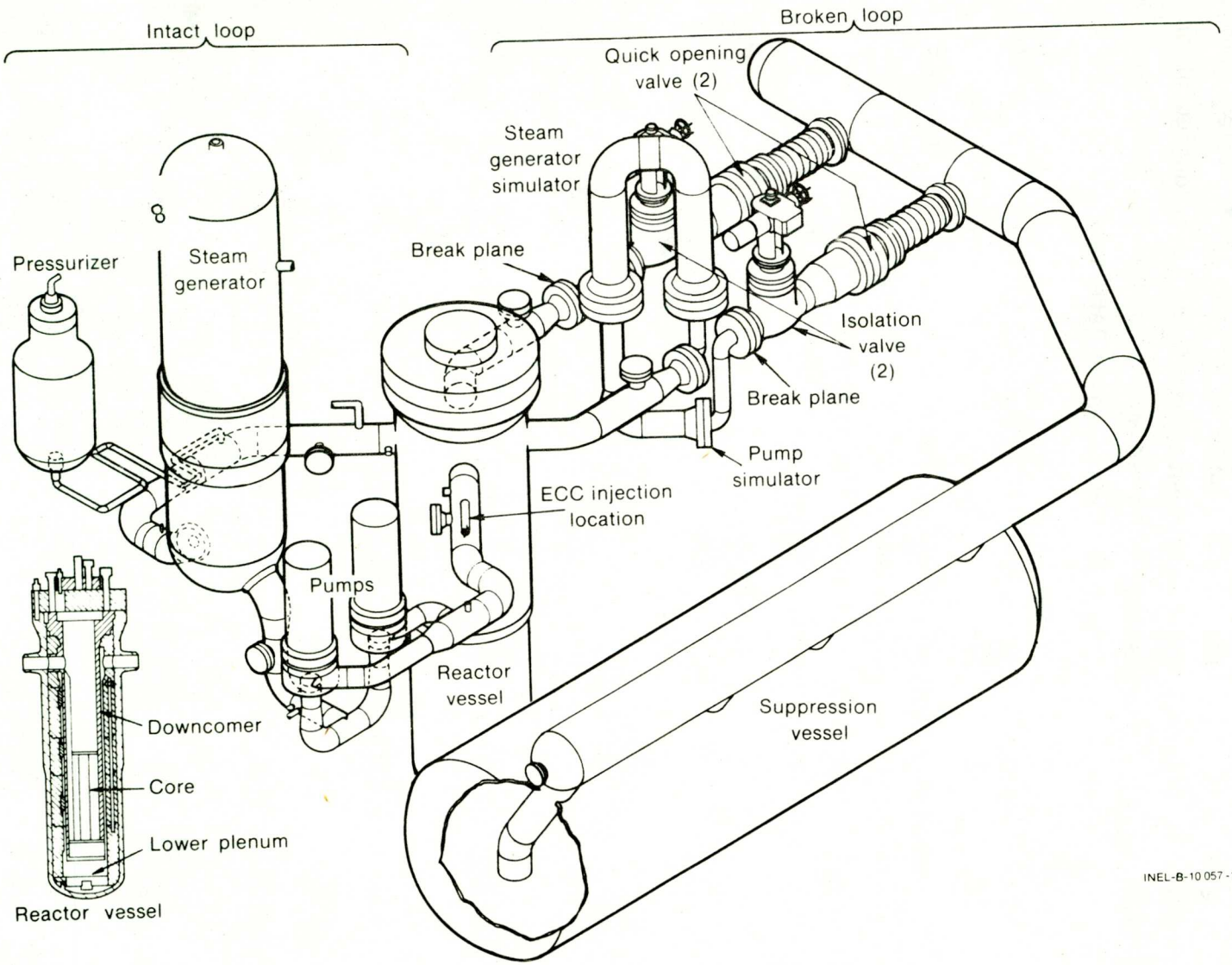

Fig. 1 Axonometric projection of LOFT system.

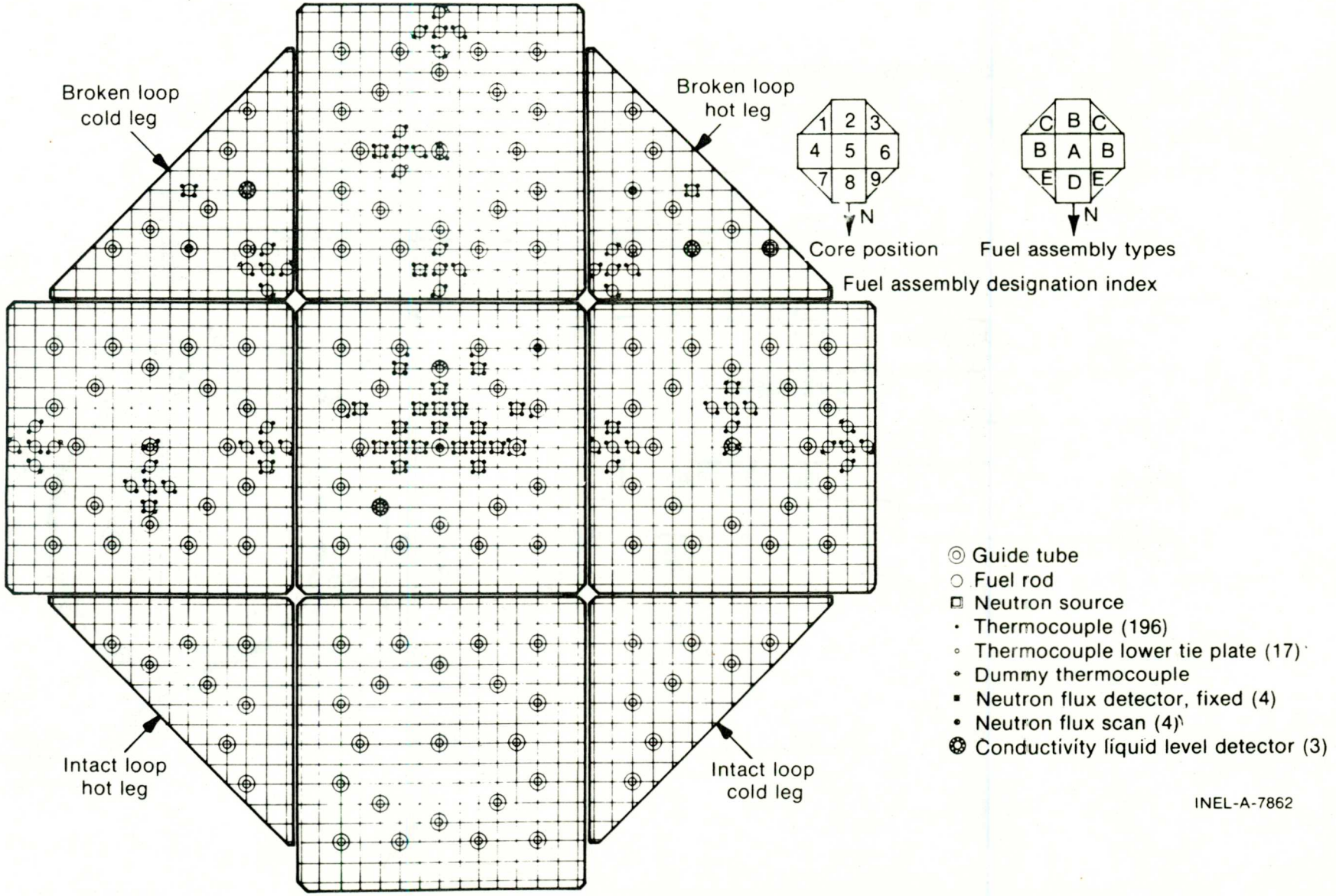

Fig. 2 LOFT core configuration and instrumentation.

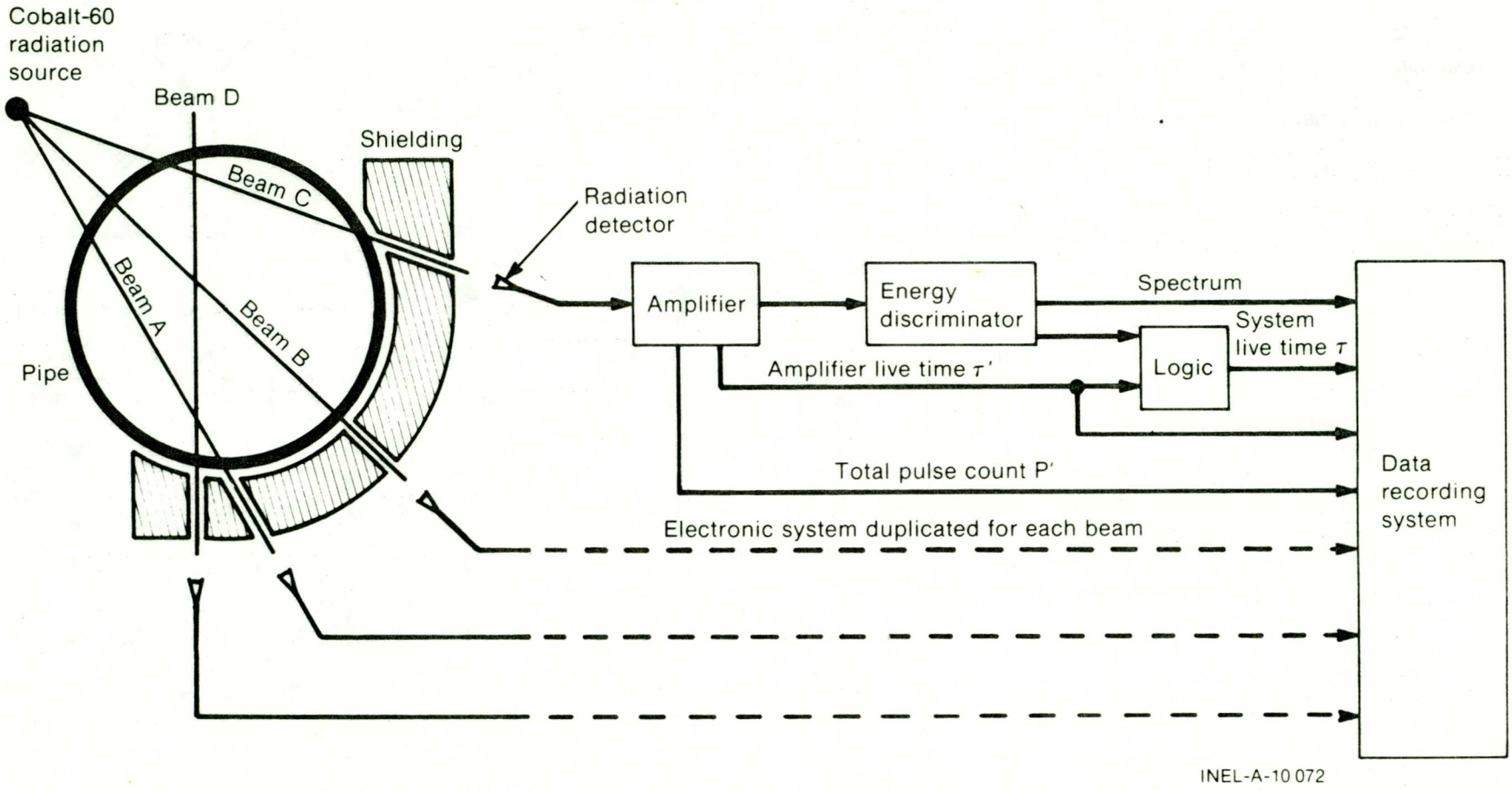

Fig. 3 Radiation-hardened gamma densitometer schematic.

TABLE I

NOMENCLATURE FOR LOFT INSTRUMENTATION

Designations for the different types of transducers:

TE	-	Temperature element	AE	-	Accelerometer
PE	-	Pressure tranducer	SE	-	Strain gage
PdE	-	Differential pressure transducer	RpE	-	Pump speed transducer
			DE	-	Densitometer
LE	-	Coolant level transducer	DiE	-	Displacement transducer
FE	-	Coolant flow transducer	ME	-	Momentum flux transducer
NE	-	Neutron detector			

Designations for the different systems, except the nuclear core:

PC	-	Primary coolant intact loop	SV	-	Suppression tank
			UP	-	Upper plenum
BL	-	Broken loop	LP	-	Lower plenum
SG	-	Steam generator	ST	-	Downcomer stalk
RV	-	Reactor vessel	IL	-	Intact loop
TA	-	Test assembly			

Designations for nuclear core instrumentation:

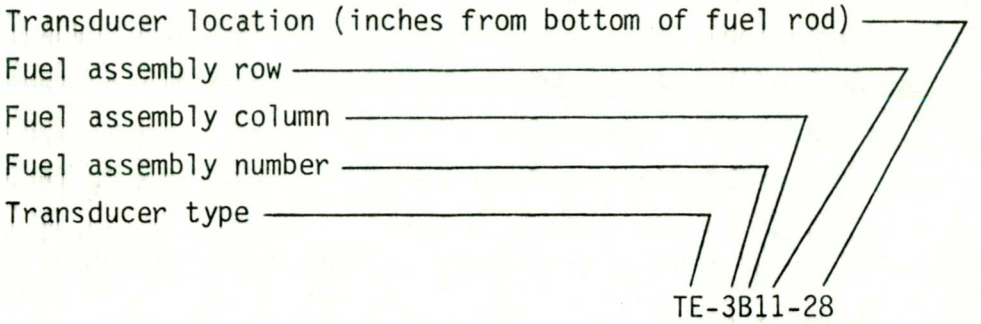

2. PLANT EVALUATION

An evaluation of plant performance is presented in this section. The discussion summarizes the initial experimental conditions, the identifiable significant events, and an evaluation of instrumentation performance for LOCE L2-2.

2.1 Initial Experimental Conditions

A summary of the specified and measured system conditions immediately prior to LOCE L2-2 blowdown initiation is given in Table II. The measured average initial temperature of the primary coolant was 569.5 K, with a range from 557.5 to 581.5 K. The measured average initial cladding temperature was 590 K, with a range from 572 to 611 K. The initial mass flow rate in the primary coolant loop was 194.2 kg/s, and the pressurizer pressure was 15.62 MPa. The initial power level yielded an MLHGR of 26.38 kW/m.

2.2 Chronology of Events

Identifiable significant events that occurred during LOCE L2-2 are listed in Table III. For LOCE L2-2, the emergency core coolant (ECC) injection from the high-pressure injection system (HPIS) and low-pressure injection system (LPIS) was initiated automatically upon receipt of a low primary system hot leg pressure coincident with a low pressurizer level trip. Accumulator ECC injection was initiated automatically when the system pressure reached 4.14 MPa. As shown in Table III, HPIS, Accumulator A, and LPIS started injection 12, 18, and 29 s after rupture initiation, respectively.

The plant protection system (PPS) initiated the reactor scram during LOCE L2-2 and would have taken control of the ECCS if the LPIS and accumulator injection had not occurred within a specified time after rupture. This condition did not occur during LOCE L2-2 and the ECCS performed as planned.

TABLE II

INITIAL CONDITIONS FOR NUCLEAR LOCE L2-2

Parameter	EOS Specified Value[2]	Measured Value
Primary Coolant System		
Mass flow rate (kg/s)[a]	--	194.2
Pressure (MPa)	15.6 ± 0.1	15.64
Temperature (T_h) (K)	587.59 ± 7.2	580.4
Boron concentration (ppm)	As required	838
Cold leg temperature (K)	--	557.7
Reactor Vessel		
Power level (MW)	--	24.88
Maximum linear heat generation rate (kW/m)	26.2	26.37
Control rod position (centimeters above full-in position)	137.2 ± 1.3	137
Pressurizer		
Steam volume (m^3)	--	0.353
Water volume (m^3)	--	0.607
Water temperature (K)	As required to establish pressure	619
Pressure (MPa)	15.6 ± 0.1	15.62
Level (cm)	113 ± 17.8	108.9
Broken Loop		
Hot leg temperature (K)	587.6 $^{+\ 0}_{-\ 44.4}$	
Near vessel	--	561.2
Near break	--	542.9

TABLE II (Continued)

Parameter	EOS Specified Value[2]	Measured Value
Broken Loop (Continued)		
Cold leg temperature (K)	563.8 $^{+\ 0}_{-\ 14}$	
Near vessel	--	555
Near break	--	538.3
Steam Generator Secondary Side[b]		
Water level (cm)	320	314
Water temperature (K)	--	553
Pressure (MPa)	--	6.35
Mass flow rate (kg/s)	--	12.67
ECC Accumulator A		
Gas volume (m^3)	--	1.05
Water volume injected (m^3)	--	1.68
Pressure (MPa)	4.22 $\pm$ 0.17	4.11
Temperature (K)	305.4 $\pm$ 8.3	300.8
Boron concentration (ppm)	3100	3301
Liquid level (m)	2.045 $\pm$ 0.03	2.01
Suppression Tank		
Liquid level (cm)	127 $\pm$ 2.54	135.07[d]
Gas volume (m^3)	--	53.3
Liquid volume (m^3)	--	31.9
Downcomer submergence (cm)[a]	--	48.73
Water temperature (K)	356 $\pm$ 3.6	352.0[d]

TABLE II (Continued)

Parameter	EOS Specified Value[2]	Measured Value
Suppression Tank (Continued)		
Pressure (gas space) (MPa)	0.086 ± 0.007	0.123[d]

(a) Calculated.

(b) Not controlled.

(c) Based on average submergence of four downcomers.

(d) Out of specification but did not affect results.

TABLE III

CHRONOLOGY OF EVENTS FOR NUCLEAR LOCE L2-2

Event	Time After Rupture Initiation (s)
LOCE L2-2 initiated	0.0
Subcooled blowdown ended[a]	∿0.1
Subcooled break flow ended[b]	∿3.5
Reactor scram signal received at control room	0.085
Control rods completely inserted	1.725
HPIS injection initiated	12
Pressurizer emptied	15
Accumulator A injection initiated	18
LPIS injection initiated	29
Lower plenum filled with liquid	35
Saturated blowdown ended	∿44
Accumulator A liquid line flow ended[c]	49
BST maximum pressure attained	67
Core volume reflooded	55

(a) End of subcooled blowdown is defined as the occurrence of the first phase transition in the system excepting the pipe break location.

(b) End of subcooled break flow is defined as the first time both break nozzles complete discharge of subcooled fluid.

(c) Flow measuring point is downstream of level indicator.

2.3 Instrumentation Performance

The performance of the instruments and the data acquisition system during LOCE L2-2 was excellent. Out of 922 instruments recorded for LOCE L2-2 approximately 872 (95%) performed satisfactorily. The instrument failures did not significantly affect the objectives of LOCE L2-2. Specific discussion concerning instrument performance is presented in Section 3.2.

The failed instruments included the three turbine meters in the drag disc-turbine transducers located in the upper plenum. The drag discs at two of these locations performed satisfactorily. Additional instruments which failed during LOCE L2-2 were DE-BL-2A and -2D at the broken loop hot leg location and DE-PC-2B and -2C at the intact loop hot leg location. At each of these locations, at least one gamma densitometer beam functioned properly which provides an indication of the coolant density. The additional failed instruments also included thermocouples and absolute pressure transducers. However, there were sufficient redundant temperature and pressure measurements at these locations to give an indication of the system behavior, and these failures did not significantly affect the results of the experiment.

3. EXPERIMENTAL RESULTS FROM LOCE L2-2

The experimental results from LOCE L2-2 are presented in this section. The results are summarized for each test objective.

3.1 Objective 1: Provide a test in which the hottest fuel pins are predicted to encounter departure from nucleate boiling (DNB) and not immediately reenter the nucleate boiling heat transfer regime to allow assessment of fuel rod-to-coolant heat transfer in the post-critical heat flux (CHF) regime.

LOCE L2-2 was predicted to encounter DNB and not immediately reenter the nucleate boiling heat transfer regime. Performance of this experiment met Objective 1.

LOFT LOCE L2-2 was conducted, within specification, for a set of initial conditions established from experimental results (thermal-hydraulic) of the LOFT nonnuclear LOCEs, experimental results of the Semiscale LOFT counterpart tests, and predictive results from the RELAP4/MOD6 and FRAP-T4 computer codes. The hottest fuel pins did encounter DNB within the time frame predicted. The fuel clad temperature response appeared to agree well with prediction in the first 3 to 4 s following LOCE L2-2 initiation. However, at approximately 4 s after rupture, rewet occurred on all fuel pins. The early rewet was predicted to occur in the cooler fuel pins located near the periphery of the core but was not predicted to occur on the hottest fuel pins. Subsequent to the rewet, the hottest fuel pins underwent several additional DNB-rewet cycles until final quench and core reflood were complete as shown in Figure 4[(a)].

(a) Further detail on the fuel rod temperature response is contained in Section 3.5.

3.2 Objective 2: Check out experimental and process instrumentation pertaining to nuclear LOCE performance.

For LOCE L2-2, 922 instruments were recorded. Of these, 872 (95%) performed successfully and provided the data necessary to meet the objectives of this experiment.

Instruments providing data pertaining specifically to the nuclear LOCE initialization and transient were the nuclear hardened gamma densitometers, traversing in-core probe (TIP), in-core self-powered neutron detectors, power range and intermediate power range instruments, and thermocouples on the fuel rod cladding. The densitometers were developed expressly for use during nuclear LOCEs. The data obtained from the densitometers provided information concerning ECC injection and ECC bypass in the presence of an external radiation field. The TIP system scans of the core power distribution prior to LOCE initiation were used to successfully determine and verify the peaking factor (2.43) and the axial power profiles during steady state operation prior to LOCE initiation. The self-powered neutron detectors provided indication of the time at which the core became subcritical due to voiding (see Figure 5) and information on steady state local linear heat generation rate[(a)]. The power range and intermediate range nuclear instruments measured, as intended, the peak and average power during steady state operation and during the core power shutdown following LOCE initiation. The core cladding thermocouples performed exceptionally well. Out of 185 cladding thermocouples 180 (97%) were operational and measured fuel rod cladding temperature in a consistent manner. The temperature measurements from the cladding thermocouples agreed with the indicated final clad quench as determined from the liquid level measurements.

(a) The instruments do not accurately follow power decline due to gamma sensitivity.

3.3 Objective 3: Determine overall performance of the LOFT facility in nuclear LOCE operation and locate any equipment/procedures that require upgrading prior to nuclear LOCE performance at higher power levels.

The overall performance of the LOFT facility during LOCE L2-2 was excellent. A few equipment/procedure problems were identified during the pre-LOCE preparations which can be easily rectified prior to performing the next LOCE.

3.4 Objective 4: Provide data to evaluate LOFT emergency core cooling system (ECCS) scaling techniques in the blowdown of a system operating at power.

The LOFT ECCS is scaled to provide an accumulator-injected-volume-to-system-volume ratio and flow duration similar to that expected in a typical large PWR. The HPIS is scaled to provide a flow-rate-to-system-volume ratio typical of PWRs. The LPIS is scaled to provide a flow-rate-to-combined-downcomer-and-core-flow-area ratio similar to that in a PWR.

ECCS performance data taken during LOCE L2-2 for the accumulator, HPIS, LPIS, and ECCS flow summation are presented in Figures 6, 7, 8, and 9, respectively. ECCS initiation times are presented in Table III along with other significant LOCE events. Preliminary analysis of the data has shown that the ECCS performed in a manner similar to that in LOFT LOCE L1-5 in which the core was not powered. Indications are that the ECCS performance indices of hot wall delay, ECC bypass, lower plenum refill rate, and core reflood rate were not adversely affected by the presence of stored energy in the core resulting from steady state power generation with an MLHGR of 26.38 kW/m. The magnitudes of the performance indices determined in the LOFT nonnuclear LOCEs are applicable to a condition of the core at power (24.88 MW) with an MLHGR of 26.38 kW/m. The core reflood rate of 0.12 m/s was the same as in LOCE L1-5 and was also nearly uniform across the core in LOCE L2-2 as was the case in

LOCE L1-5. The liquid level plots presented in Figures 10 through 14 help indicate reflood rate.

3.5 Objective 5: Determine LOFT fuel rod temperature response in a 26.2 kW/m maximum linear heat generation rate (MLHGR) double-ended cold leg break LOCE.

The LOFT fuel rod temperature response in a 26.38 kW/m MLHGR during a double-ended cold leg break is illustrated in Figures 15 through 28. Table IV presents all cladding initial temperatures, peak cladding tempertures, time to first DNB, time to peak cladding temperature, and time to final quench. The measured peak cladding temperature was 789 K, which occurred in the center module, 0.76 m from the core bottom, on Fuel Rod 5J4.

The general thermal behaviors of all fuel rods in the central fuel module were similar. Initial DNB was measured at approximately 1.5 s[(a)], followed by the cladding temperature rapidly rising to a maximum measured temperature between 4 and 6 s. Between 6 and 7 s, rewet of the cladding started at the bottom of the fuel rod and progressed upward and rapidly cooled the cladding. At about 12 to 16 s after rupture, most rods in the center module experienced a dryout resulting in a small temperature increase. The rods were then rewet progressively from top to bottom and cooled to the core saturation coolant conditions by 21 s. Another dryout occurred between 21 and 22 s causing very small cladding temperature increases along the higher power portions of the rod. Again the rods were rewet, progressing from top to bottom, and cooled by 25 s. Between 30 and 35 s a gradual temperature increase along the entire rod length was measured. The rod was then cooled by a reflood quench starting at the bottom and progressing upward. The total core was quenched between 35 and 40 s. Figures 15 through 20 show the measured cladding temperature along the axial length

---

(a) All times are relative to the initiation of blowdown valve opening.

TABLE IV

SUMMARY OF CORE TEMPERATURE RESPONSE CHARACTERISTICS

Instrument	$T_{initial}$(K)	T_{peak}(K)	t_{DNB}(s)[a]	t_{peak}(s)	t_{quench}(s)
TE-1A11-030	594	663	4	6.6	36.7[b]
TE-1B10-037	592	596	6.2	6.9	36.8
TE-1B11-028	592	648	4.8	6.5	38.8
TE-1B11-032	596	652	4.3	6.7	38.8
TE-1B12-026	593	671	3.4	6.5	36.8
TE-1C11-021	581	632	3.8	6.2	36.8
TE-1C11-039	599	601	6.4	7.7	38.9
TE-1F7-015	576	579	5.9	6.5	34.7
TE-1F7-021	577	587	5.9	6.6	36.7
TE-1F7-026	579	595	5.6	6.8	36.7
TE-1F7-030	586	602	5.3	6.8	36.7
TE-2E8-011	577	593	0[c]	0.1	34.7
TE-2E8-030	591	594	0	-9.2	38.8
TE-2E8-045	596	601	0	-7.4	43.7
TE-2F7-015	577	580	0	0.3	37
TE-2F7-037	589	592	0	-0.6	38.8
TE-2F8-028	586	590	0	-7.1	42
TE-2F8-032	592	595	0	-8.4	41
TE-2F9-026	586	590	0	-1.2	42
TE-2F9-041	592	593	0	-2.1	42
TE-2G02-030	581	585	0	-6.7	39
TE-2G08-021	586	589	0	-0.6	36.8
TE-2G08-039	589	592	0	-8.1	38.9
TE-2G14-011	582	704	1.6	5.3	34.7
TE-2G14-030	604	696	3.3	6.4	41.5
TE-2G14-045	606	679	2	6.1	43.7
TE-2H01-037	576	580	0	0.2	39
TE-2H02-028	577	585	9.9	0.1	39
TE-2H02-032	579	581	6.8	-0.1	38.8
TE-2H03-026	580	583	0	0.1	36.7
TE-2H13-021	591	594	0	-6.7	36.7
TE-2H13-049	601	604	0	-7.3	44
TE-2H14-028	598	672	2.8	5.1	42
TE-2H14-032	601	706	2.1	6.4	41.5
TE-2H15-026	599	746	2	5.9	36.8
TE-2H15-041	601	665	1.9	6.3	38.9
TE-2I02-021	580	589	0	0.1	36.7
TE-2I02-039	577	580	0	0.3	38.8
TE-2I14-021	588	691	3.8	6.3	37
TE-2I14-039	599	611	4	5.7	38.9

TABLE IV (Continued)

Instrument	$T_{initial}$(K)	T_{peak}(K)	t_{DNB}(s)[a]	t_{peak}(s)	t_{quench}(s)
TE-3A11-030	(d)				
TE-3B10-037	592	595	6.5	7	39
TE-3B11-028	595	631	4.3	6.8	41.5
TE-3B11-032	604	653	4.4	6.6	39.2
TE-3B12-026	599	636	4.5	6.5	38.7
TE-3C11-021	579	612	4.7	6.2	37.2
TE-3C11-039	600	602	5.1	6	39
TE-3F7-015	575	597	5.5	6.4	35.3
TE-3F7-021	577	596	5.2	5.9	36.6
TE-3F7-026	579	608	5.3	6.8	36.8
TE-3F7-030	583	622	4.7	6.9	36.9
TE-4E8-011	576	580	0	0.4	N/A
TE-4E8-030	591	594	0	-9.6	36.9
TE-4E8-045	599	602	0	-4.7	38.9
TE-4F7-015	574	580	0	0.3	N/A
TE-4F7-037	584	586	0	-0.5	38.8
TE-4F8-028	588	593	0	-5.6	36.8
TE-4F8-032	591	593	0	-4.1	38.8
TE-4F9-026	586	588	0	0.1	36.8
TE-4F9-041	594	597	0	-6.9	39.9
TE-4G02-030	583	586	6.5	8	36.8
TE-4G08-021	582	586	0	-0.5	36.7
TE-4G08-039	595	598	0	-7.4	38.9
TE-4G14-011	592	745	1.8	5.4	34.6
TE-4G14-030	602	745	1.9	6.6	36.9
TE-4G14-045	603	670	1.8	6	38.9
TE-4H01-037	578	582	0	0.4	39.2
TE-4H02-028	578	582	5.3	6	36.9
TE-4H02-032	581	585	6.5	7.1	37.1
TE-4H03-026	579	594	6.0	6.7	36.8
TE-4H13-015	(d)				
TE-4H13-037	606	608	0	5.1	38.8
TE-4H14-028	600	745	1.5	6.4	36.8
TE-4H14-032	601	741	1.7	5.9	37
TE-4H15-026	606	766	1.9	6.4	36.7
TE-4H15-041	606	717	1.6	6.6	38.9
TE-4I02-021	574	587	5.6	6.6	36.7
TE-4I02-039	583	590	5.2	6	38.8
TE-4I14-021	597	722	2.1	5.1	36.7
TE-4I14-039	608	700	1.3	6.8	38.9

TABLE IV (Continued)

Instrument	$T_{initial}$(K)	T_{peak}(K)	t_{DNB}(s)[a]	t_{peak}(s)	t_{quench}(s)
TE-5D6-030	600	776	1.7	6.2	36.9
TE-5D6-032	604	764	1.6	6.4	36.9
TE-5D6-037	604	757	1.7	6.6	38.8
TE-5D6-039	606	762	1.9	6.3	38.8
TE-5E8-002	(d)				
TE-5E8-015	575	747	1.5	5.4	37
TE-5E8-034.5	598	715	1.7	6.3	37
TE-5E8-049	610	718	1.5	6.7	38.9
TE-5F4-015	585	746	1.5	3.6	39
TE-5F4-021	599	764	1.4	5.2	38.7
TE-5F4-026	602	745	1.8	5.6	42
TE-5F4-030	604	788	1.9	6.3	44
TE-5F7-005	(d)				
TE-5F7-021	576	642	1.4	6.4	36.6
TE-5F7-039	594	742	1.6	6.3	38.8
TE-5F7-054	(d)				
TE-5F8-024	599	773	1.2	4.7	36.7
TE-5F8-028	597	786	1	4	36.9
TE-5F8-032	599	753	1.6	6.7	38.8
TE-5F8-037	604	751	1.5	6.5	38.8
TE-5F9-011	583	719	1.6	5.6	34.6
TE-5F9-030	599	748	1.6	5.3	36.8
TE-5F9-045	609	737	1.7	6.6	43.8
TE-5F9-062	600	665	2.2	6.7	44
TE-5G6-011	581	714	1.5	3.6	31.9
TE-5G6-030	601	749	1.6	5.1	36.8
TE-5G6-045	605	743	1.6	6.6	38.9
TE-5G6-062	598	664	2.2	6.7	44.5
TE-5G8-008	582	706	1.7	3.7	34.6
TE-5G8-026	594	770	1.4	6.5	36.8
TE-5G8-041	605	731	1.6	6.6	38.8
TE-5G8-058	601	675	2	6.8	43.9
TE-5H5-002	566	637	2.2	3.6	31.7
TE-5H5-015	582	759	1.5	5.4	35.5
TE-5H5-034.5	599	733	1.7	5.2	37.1
TE-5H5-049	605	705	1.7	5.6	38.9
TE-5H6-024	593	759	1.3	4.1	36.7
TE-5H6-028	599	762	1.9	6.5	36.8
TE-5H6-032	603	762	1.6	6.3	36.9
TE-5H6-037	604	747	1.3	6.2	37

TABLE IV (Continued)

Instrument	$T_{initial}$(K)	T_{peak}(K)	t_{DNB}(s)[a]	t_{peak}(s)	t_{quench}(s)
TE-5H7-008	585	702	1.7	5.3	34.6
TE-5H7-026	598	771	1.6	5.1	36.7
TE-5H7-041	603	740	1.6	5.9	38.8
TE-5H7-058	601	672	2.3	6.9	43.8
TE-5I6-005	571	700	1.8	3.7	31.8
TE-5I6-021	597	782	1.4	3.7	36.7
TE-5I6-039	604	756	1.4	6.4	38.8
TE-5I6-054	604	690	1.7	6.4	38.9
TE-5I8-008	582	704	2.1	5.5	34.6
TE-5I8-026	603	772	1.7	5.2	36.8
TE-5I8-041	607	738	1.5	6.3	38.8
TE-5I8-058	603	679	2	6.8	43.8
TE-5J4-015	587	751	1.5	3.7	36.6
TE-5J4-021	601	769	1.7	5.5	41
TE-5J4-026	603	762	1.5	4.8	42
TE-5J4-030	604	789	1.5	5.8	42.8
TE-5J7-011	581	719	1.6	5.7	34.8
TE-5J7-030	602	747	1.6	6.1	36.7
TE-5J7-045	610	734	1.4	6.1	38.9
TE-5J7-062	601	663	2.1	6.4	44.1
TE-5J8-024	604	765	1.3	4.7	36.7
TE-5J8-028	601	771	1.6	6.4	36.8
TE-5J8-032	610	767	0.5	5.7	36.9
TE-5J8-037	601	748	1.7	6.1	39
TE-5J9-005	572	670	1.7	3.6	31.9
TE-5J9-021	582	774	1.4	3.7	36.7
TE-5J9-039	(d)				
TE-5J9-054	604	695	1.8	6.7	39.1
TE-5K8-002	565	645	1.9	3.6	31.7
TE-5K8-015	593	751	1.7	5.2	34.8
TE-5K8-034.5	602	726	1.7	5.8	36.8
TE-5K8-049	605	719	1.7	6.7	38.9
TE-5L6-030	603	772	1.7	5.7	38.8
TE-5L6-032	607	757	1.7	5.9	38.8
TE-5L6-037	607	737	1.6	6.5	39.2
TE-5L6-039	605	729	2	6.6	39.2
TE-6E8-011	580	586	0	-1.7	34.6
TE-6E8-030	592	600	0	-0.6	38.7
TE-6E8-045	596	598	0	-4.2	39.2
TE-6F7-015	577	587	0	-2.9	37.5

TABLE IV (Continued)

Instrument	$T_{initial}$(K)	T_{peak}(K)	t_{DNB}(s)(a)	t_{peak}(s)	t_{quench}(s)
TE-6F7-037	590	594	0	0.1	38.8
TE-6F8-028	586	590	0	-4.5	39
TE-6F8-032	589	592	0	-4.2	41.5
TE-6F9-026	583	587	0	0.1	39
TE-6F9-041	590	595	0	-2.3	38.9
TE-6G02-030	580	584	0	-2.2	39
TE-6G08-021	584	587	0	-10.1	36.7
TE-6G08-039	591	594	0	-3.7	38.9
TE-6G14-011	588	707	1.6	5.6	34.7
TE-6G14-030	605	709	1.6	3.3	39.1
TE-6G14-045	607	669	1.8	4.1	37
TE-6H01-037	576	580	0	0.3	36.8
TE-6H02-028	579	584	0	-1.7	38.8
TE-6H02-032	578	583	0	-7.7	38.8
TE-6H03-026	582	585	0	-2	36.7
TE-6H13-015	583	630	2.4	3.2	36.6
TE-6H13-037	601	628	1.8	2.4	38.8
TE-6H14-028	596	700	1.9	3.4	38.7
TE-6H14-032	605	729	1.9	4.1	38.8
TE-6H15-026	605	748	2	5.5	35.1
TE-6H15-041	607	682	1.4	4.5	36.9
TE-6I02-021	575	581	0	0.4	37
TE-6I02-039	581	583	0	-5.4	36.9
TE-6I14-021	593	742	1.6	5.1	41.5
TE-6I14-039	606	664	1.4	2.2	36.9

(a) Time to first DNB.

(b) Time to final quench.

(c) Zero indicates rod did not enter first DNB.

(d) Instrument failed.

of the fuel rods clustered about Fuel Rod 5F8 (center module, see Figure 2). For comparison, the predicted temperature responses for the peak power rod are also shown in the figures.

Figure 15 shows the details of the initial DNB and cladding temperature rise. Initial DNB occurred near the rod peak power location and within 0.5 s occurred over the entire length of the rod. The cladding temperature rise followed the predicted cladding temperature near the peak power locations for the first 1 to 2 s but then reached peak temperatures that are significantly less than those predicted. Figure 16 shows the initial rewetting of the rods progressing from the bottom to the top of the rods. This rewet cooled the entire fuel rod in less than 2 s ($6 < t < 8$ s). At present, the fluid behavior causing the rewet response is under further investigation.

Figure 17 shows a time sequence of the dryout and subsequent heatup between 10.5 and 16.5 s. Figure 18 shows the rewetting of the fuel rods which initially occurred at a higher rod elevation and progressed downward. The peak power location cladding temperature was reduced again to the coolant temperature within 0.5 s after rewet initiation.

Figure 19 shows the next dryout phase which occurred over a much smaller axial length than is shown in Figure 17. Again, rewet occurred from the higher to lower elevations which cooled the elevated cladding temperatures in approximately 1.5 s.

Figure 19 shows a gradual cooling of the entire length of the fuel rods during times ranging from 25 to 30 s. However, from 30 to 35 s, the entire length of the cladding gradually heated up, the cladding temperatures being axially uniform as was observed in the isothermal LOCE L1-5. Figure 20 shows the quench due to bottom reflooding of the fuel rods which progressed from the bottom to the top of the fuel rod. The reflood characteristics of LOFT are presented in Section 3.9.

There is no evidence to indicate that the low cladding temperature resulted from differences in actual and predicted fuel rod, fuel pellet,

or fuel-rod-to-cladding thermal conductivities. In fact, the initial rise time and rate compared well with the predictions.

The same cladding temperature response described above can be seen in three-dimensional plots presented in Figures 21 through 23. Additional cladding temperature overlays are presented in Figures 24 through 28.

Predictions made by RELAP4 and TRAC codes are presented in Figures 27 through 28. Early rewet of the hot rods was not predicted in either code. The reason for the variations will be determined by further analysis.

3.6 Objective 6: Determine blowdown thermal-hydraulic response at 67% nominal hot-leg-to-cold-leg temperature difference of 23.9 K.

The depressurization curve which characterizes the general behavior of blowdown is presented in Figure 29. The general nature of the data is similar to that from Semiscale Test S-06-2, which is the LOFT L2-2 counterpart test. Also shown are the RELAP4 and TRAC pretest predictions which bracket the measured LOFT behavior. The RELAP4 code predicted the general nature of the thermal-hydraulics trends in most of the LOFT primary coolant system and blowdown system. As an example, the predicted and measured momentum flux in the broken loop cold leg are compared in Figure 30. Additional comparisons are shown and discussed in Section 3.9.

The addition of core heat did not significantly affect the intact and broken loop system thermal-hydraulic behavior. Pressure, temperature, and density are very similar between LOFT isothermal LOCE L1-5 and nuclear LOCE L2-2.

As the pressure in the vessel decreased after the initiation of rupture, the first significant change in the system behavior occurred

at about 100 ms. This is probably due to the first occurrence of quality in the coolant which has the highest local temperature (end of subcooled blowdown).

The second significant event, outside the core, altered the depressurization rate at approximately 3.5 to 4 s as shown in Figure 31. The change in depressurization rate signifies the end of subcooled discharge and appeared to be when two-phase fluid conditions occurred in the broken loop cold leg. Saturated blowdown continued to 44 s when reflood took over as discussed in Section 3.9. Figures 29 through 37 present data showing the LOFT thermal-hydraulic response.

The early rewet that occurred at about 4 s on all fuel rods in DNB is considered at this time to be hydraulically induced. The origins of this phenomenon may lie in the nonisothermal conditions that exist in a reactor primary coolant system as a result of the core being at power. Analyses are currently underway to understand this phenomenon.

It should be noted that rewet is a threshold phenomenon. The RELAP4 code predicted such a threshold, as indicted by the lower power fuel rod temperature predictions shown in Figure 38. However, either the threshold location inaccurately predicted or a variation in hydraulics significant enough to cross this threshold occurred in the test. Therefore, this phenomenon of early rewet may not exist in higher power tests.

3.7 Objective 7: Determine if any clad perforation occurs in a 26.2 kW/m MLHGR double-ended cold leg break LOCE.

Clad perforation did not occur during LOCE L2-2. Peak clad temperature for LOCE L2-2 was 810 K, which is below the threshold for clad deformation as seen in Figure 39. Chemistry samples taken after the experiment from the suppression system, which receives blowdown effluent during a LOCE, indicated no fission products were released into the

effluent. The lack of fission products in the blowdown suppression system is another strong indication that no clad perforation occurred during LOCE L2-2

3.8 Objective 8: Provide integral nuclear system code verification data on a low-to-intermediate power double-ended cold leg break.

LOCE L2-2 provides to the nuclear community a large quantity of data for code assessment on a low-to-intermediate power double-ended cold leg break. Examples of data provided by LOCE L2-2 for code assessment are presented in Figures 27 through 37.

Pretest predictions using RELAP4/MOD6 were performed for LOCE L2-2. A discussion of the predictions and modeling techniques are described in Reference 4. Also, pretest predictions of LOCE L2-2 were provided by the Los Alamos Scientific Laboratory using the TRAC code. A detailed discussion of the TRAC modeling approach and results from their calculations can be found in Reference 8. Comparisons of selected RELAP4 and TRAC calculation results with experimental data are shown in Figures 27, 28, and 29 and 31 through 37 as examples of types of data that can be used for code assessment.

3.9 Objective 9: Determine LOFT reflood characteristics at 26.2 kW/m MLHGR initial condition.

LOCE L2-2 has provided the first large scale reflood data on a nuclear system. The reflood behavior was generally as expected with a reflood rate of ~0.12 m/s as determined from the liquid level plots presented in Figures 10, 11, 12, 13, and 14. The reflood rate was approximately the same as that in nonnuclear LOCE L1-5. The reflood appears to be nearly uniform across the core in LOCE L2-2 as was the case in LOCE L1-5. The core was completely covered at 55 s after rupture initiation. The uniformity of the rate of reflood across the core, as indicated by liquid level detectors and core thermocouples, suggests that the power distribution is not a significant influence at power levels of 26.2 kW/m and peaking factors of up to 2.43.

4. CONCLUSIONS

The conduct of LOFT LOCE L2-2 and the experimental data acquired concerning integral systems phenomena associated with loss of coolant are considered to have met the objectives as defined by the EOS and discussed in Section 3.0. For the first time, experimental information was obtained on a nuclear reactor system at power conditions undergoing a loss of primary coolant. The information, in addition to being new, was very interesting because of the unexpected phenomena evidenced in the data concerning the thermal response of the core and the thermal-hydraulics in the core region. The experimental data obtained from LOCE L2-2 will be extensively analyzed in the forthcoming months to determine the causes of the much lower than expected fuel clad temperature rise and the hydraulic behavior in the core region. Conclusions based on the preliminary analyses and test assessment are:

(1) The ECCS performance was not adversely affected by the presence of a heated core. The performance indices of hot wall delay, ECC bypass, lower plenum refill rate, and core reflood rate were essentially unchanged from the values determined in LOFT nonnuclear LOCE L1-5.

(2) Fuel clad temperature rise was much lower than predicted for the core conditions of 26.2 kW/m and peaking factor of 2.43. The fuel clad temperature rise was hydraulically limited by early rewet before ECCS initiation. Subsequent DNB-rewet cycles before and during core reflood indicate a strong ECC influence on fuel clad temperature.

(3) The thermal-hydraulic behavior in the primary coolant system, excepting the core region, continued to be well predicted by the computer codes.

5. DATA PRESENTATION

This section presents selected, preliminary data from LOCE L2-2. LOCE L2-2 data are overlayed with data from Semiscale LOFT counterpart Test S-06-2, LOCE L2-2 pretest predictions using the RELAP4/MOD6, FRAP-T4 and TRAC computer codes. A listing of the data plots is presented in Table V.

TABLE V

LIST OF DATA PLOTS

Figure Number	Title	Measurement[a] Identification	Page Number
4	Temperature of cladding of Fuel Module 5, Rod G6, Rod G8, and Rod H5.	TE-5G6-030 TE-5G8-26 TE-5G8-41 TE-5H5-034.5	33
5	Relative local heat generation rate from self-powered neutron detector in Module 4.	NE-4H8-33.5	33
6	Flow rate in ECCS Accumulator A discharge line, high range.	FT-P120-36-1	34
7	Flow rate in ECCS HPIS Pump A discharge line.	FT-P128-104	34
8	Flow rate in ECCS LPIS Pump A discharge line.	FT-P120-85	35
9	Volumetric flow rate of ECC into cold leg injection line calculated from FT-P120-36-1 and -85 and FT-P128-104.		35
10	Liquid level in downcomer and lower plenum under broken loop.	LE-1ST	36
11	Liquid level in core in Fuel Module 1.	LE-1F10	36
12	Liquid level in core in Fuel Module 3.	LE-3F10	37
13	Liquid level in core in Fuel Module 5.	LE-5E11	37
14	Liquid level in upper plenum above Fuel Module 3.	LE-3UP	37
15	Initial DNB and rise to peak cladding temperature during 0 to 5 s after rupture (center module cluster about Fuel Rod 5F8).		38

TABLE V (continued)

Figure Number	Title	Measurement Identification[a]	Page Number
16	Initial rewet (from bottom) during 6 to 9 s after rupture (center module cluster about Fuel Rod 5F8).		39
17	First dry-out during 10.5 to 16 s after rupture (center module cluster about Fuel Rod 5F8).		40
18	Second rewet (from top) during 16.5 to 19 s after rupture (center module cluster about Fuel Rod 5F8).		41
19	Second dry-out and third rewet (from top) during 21 to 27 s after rupture (center module cluster about Fuel Rod 5F8).		42
20	Sight heatup prior to reflood quench (from bottom) during 28 to 38 s after rupture (center module cluster about Fuel Rod 5F8).		43
21	Three-dimensional axial profile of cladding temperature of Fuel Module 5.	TE-5G8-58 TE-5F9-45 TE-5E8-34.5 TE-5G8-26 TE-5F9-11 TE-5LP-2	44
22	Three-dimensional axial profile of cladding temperature of Fuel Module 5.	TE-5UP-7 TE-5I8-58 TE-5J7-45 TE-5K8-34.5 TE-5I8-26 TE-5J7-11 TE-5LP-3	45
23	Three-dimensional radial profile at 0.76-m core elevation.	TE-6I2-30 TE-6I14-30 TE-5D6-30 TE-4G8-30	46

TABLE V (continued)

Figure Number	Title	Measurement[a] Identification	Page Number
24	Temperature of cladding of Fuel Module 5, Rod D6.	TE-5D6-30 TE-5D6-32 TE-5D6-37 TE-5D6-39	47
25	Temperature of cladding of Fuel Module 1, Rod B11 and of Fuel Module 4, Rods G2 and G14.	TE-1B11-28 TE-1B11-32 TE-4G02-30 TE-4G14-30	47
26	Temperature of cladding of Fuel Module 4, Rods H02, H14, F8 and Fuel Module 6, Rods 6H02 and 6H14.	TE-4H02-028 TE-4F8-028 TE-4H14-28 TE-6H02-028 TE-6H14-028	48
27	Temperature of cladding of Fuel Module 5, Rod F4 for LOCE L2-2 data, TRAC, and RELAP4 calculations.	TE-5F4-15	48
28	Temperature of cladding of Fuel Module 5, Rod F4 for LOCE L2-2 data, TRAC, and RELAP4 calculations.	TE-5F4-21	49
29	Pressure in upper plenum for Semiscale Test S-06-2, LOFT LOCE L2-2), RELAP4, and TRAC.	PE-1UP-1A	49
30	Momentum flux in broken loop cold leg for RELAP4 and LOCE L2-2 data.	ME-BL-1B	50
31	Pressure in intact loop cold leg.	PE-PC-1	50
32	Density in broken loop cold leg.	DE-BL-1B	51
33	Density in intact loop cold leg.	DE-PC-1B	52
34	Temperature in broken loop cold leg.	TE-BL-1B	53
35	Temperature in intact loop cold leg.	TE-PC-1B	53

TABLE V (continued)

Figure Number	Title	Measurement[a] Identification	Page Number
36	Pressure in broken loop cold leg.	PE-BL-1	54
37	Pressure in intact loop cold leg.	PE-PC-1	54
38	Temperature of cladding on Fuel Module 3, Rod B12 for LOCE L2-2 data and RELAP4.	TE-3B12-026	55
39	Modes of cladding deformation at different pressures and temperatures maintained for 15 s.		55

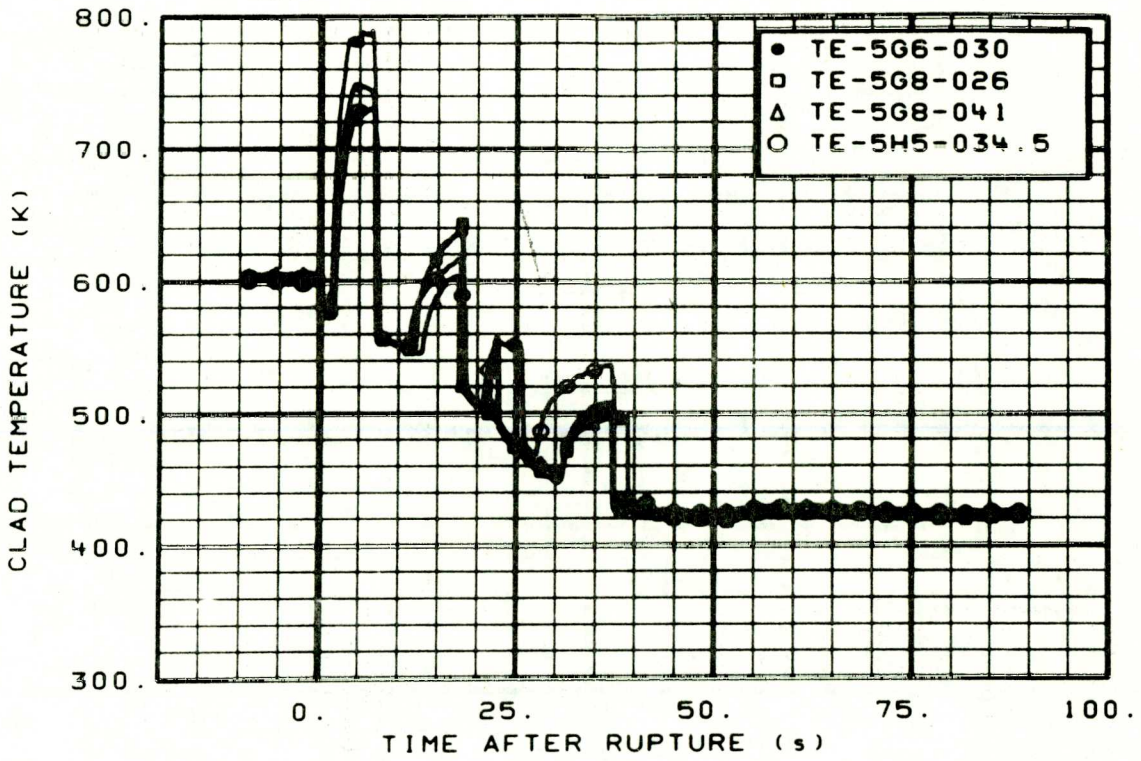

Fig. 4 Temperature of cladding of Fuel Module 5, Rod G6, Rod G8, and Rod H5 (TE-5G6-030, TE-5G8-26 and -41, and TE-5H5-034.5).

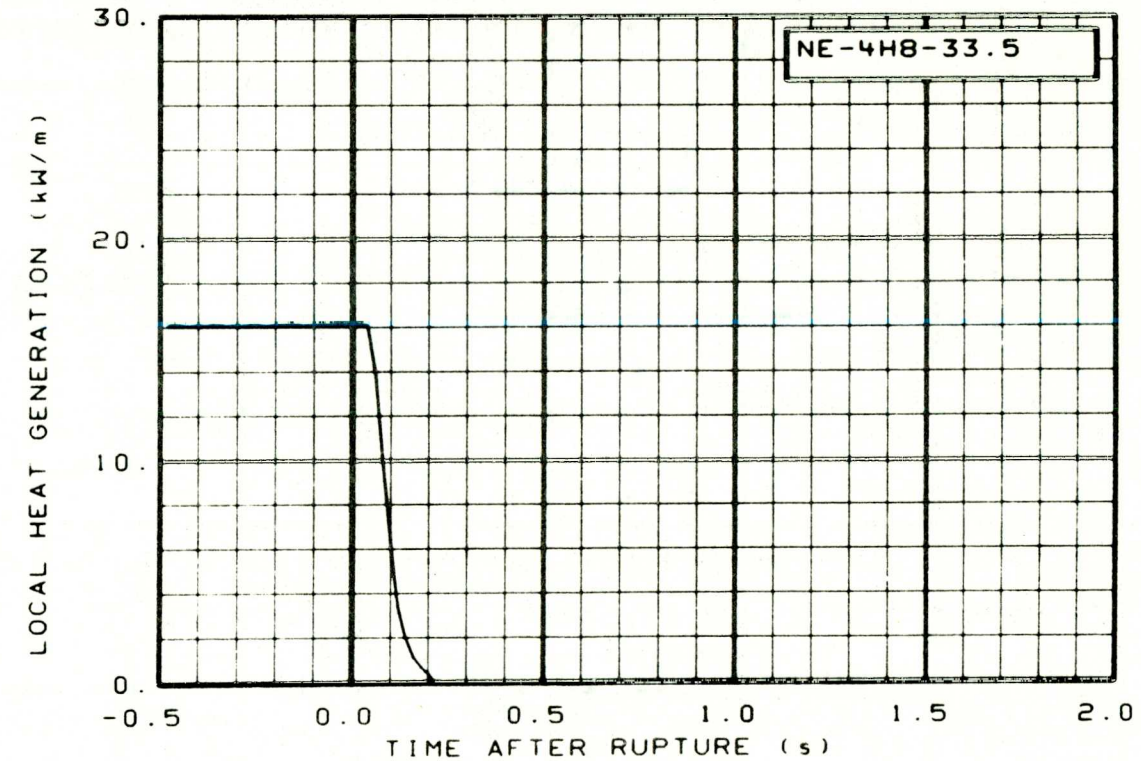

Fig. 5 Relative local heat generation rate from self-powered neutron detector (NE-4H8-33.5) in Module 4.

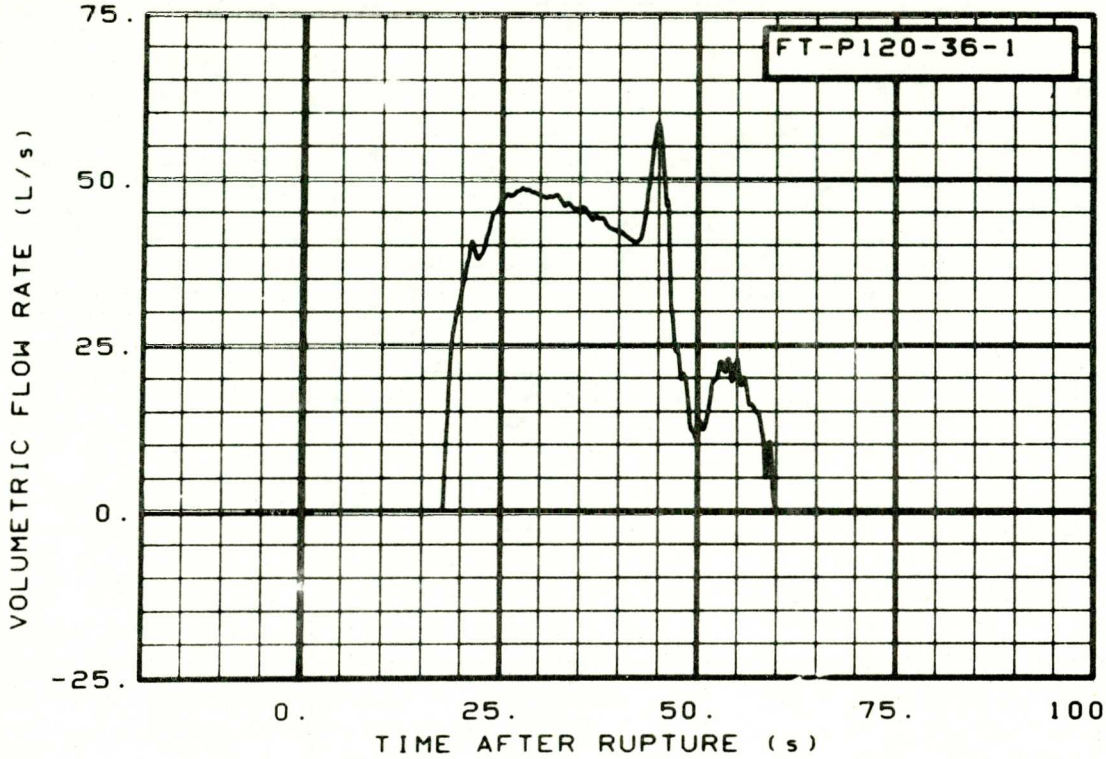

Fig. 6 Flow rate in ECCS Accumulator A discharge line, high range (FT-P120-36-1).

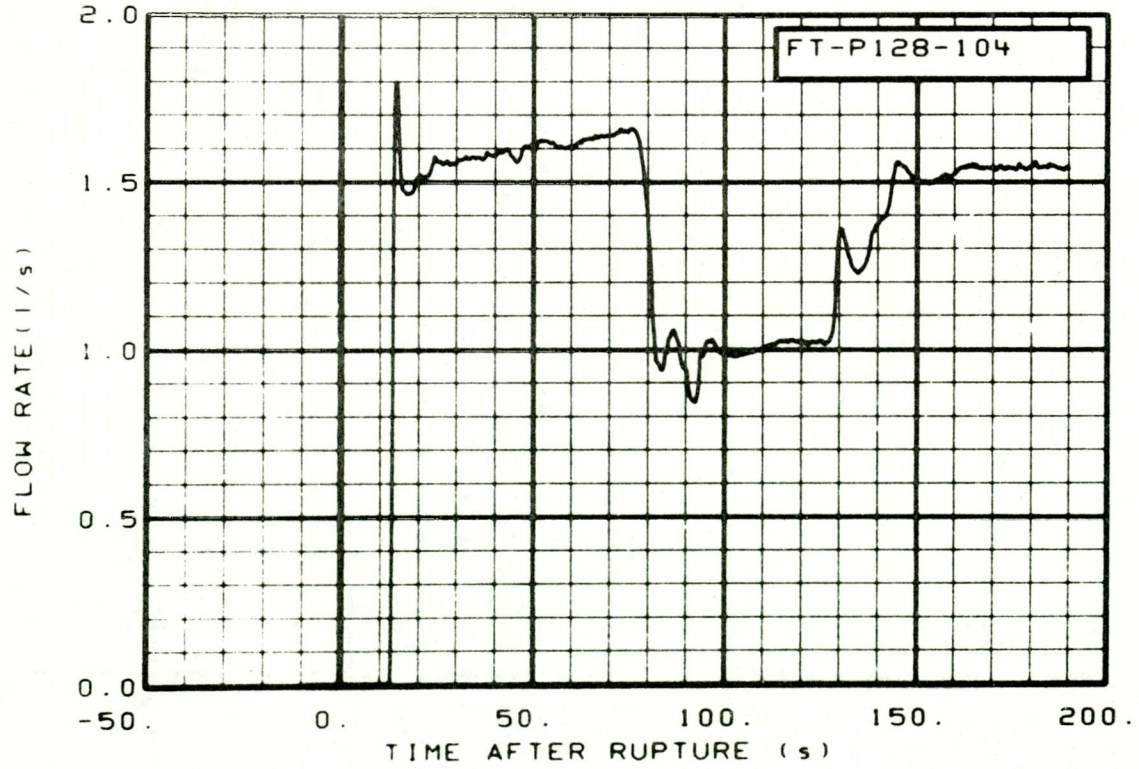

Fig. 7 Flow rate in ECCS HPIS Pump A discharge line (FT-P128-104).

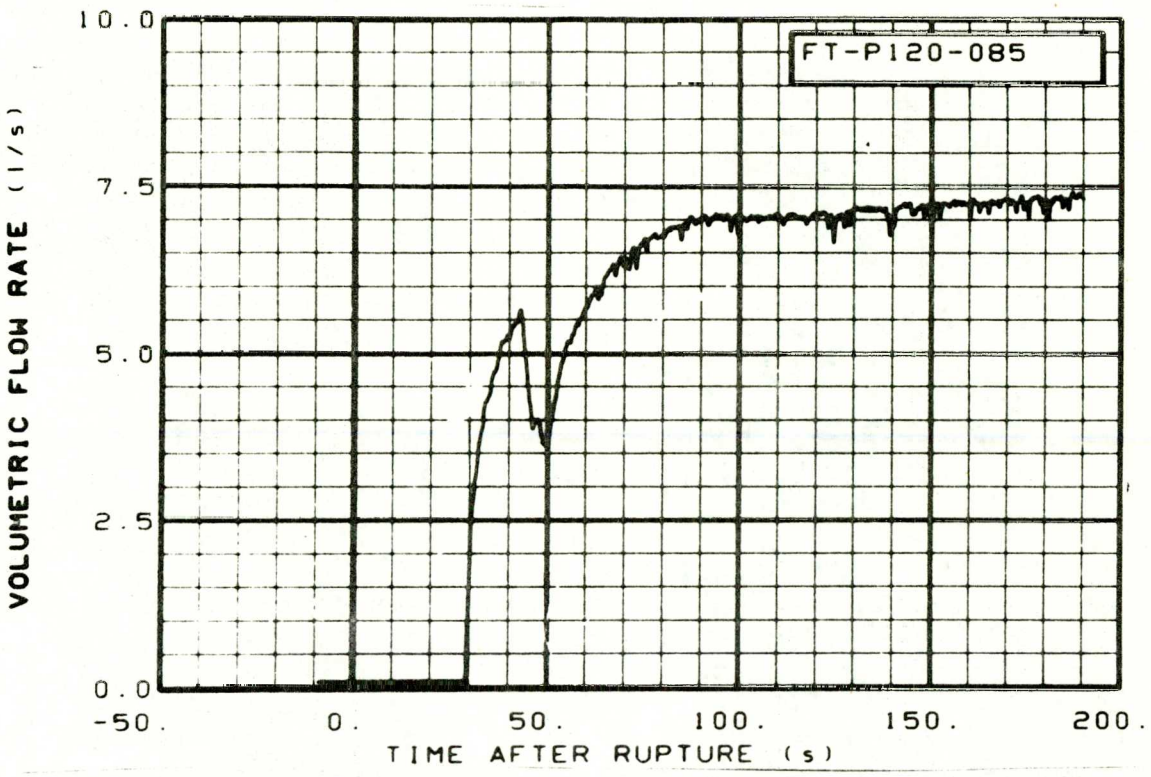

Fig. 8 Flow rate in ECCS LPIS Pump A discharge line (FT-P120-85).

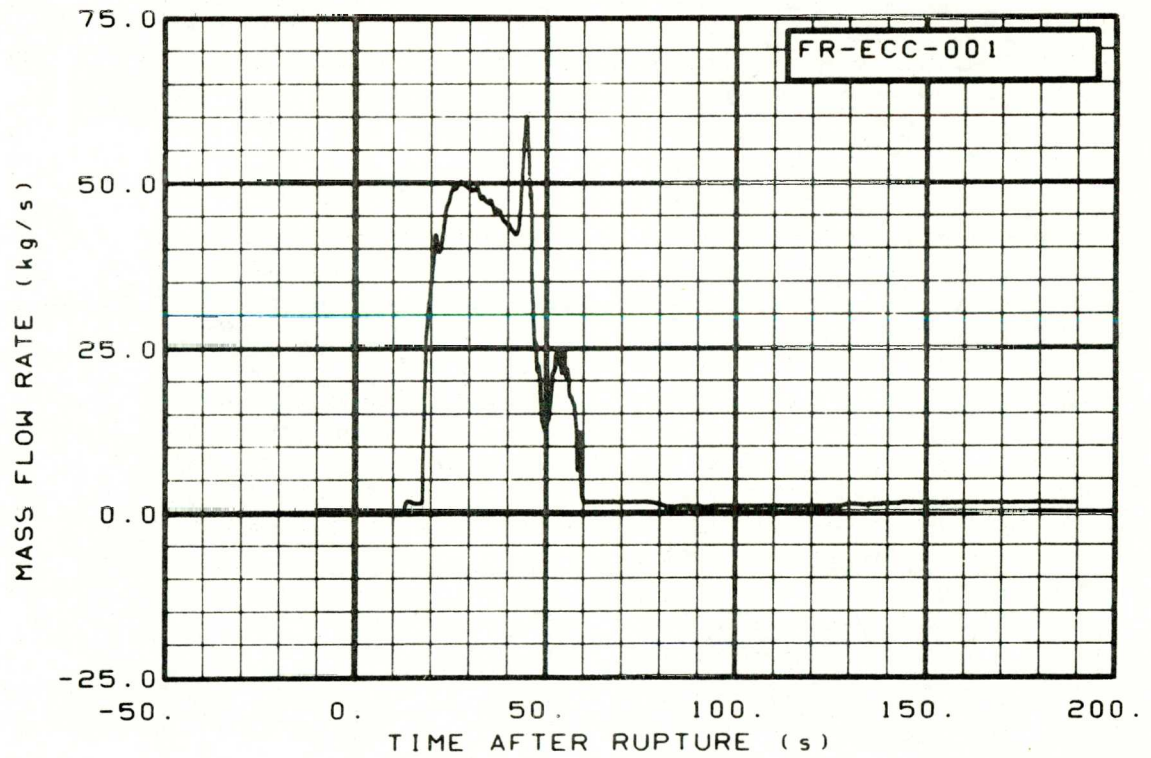

Fig. 9 Volumetric flow rate of ECC into cold leg injection line calculated from FT-P120-36-1 and -85 and FT-P128-104.

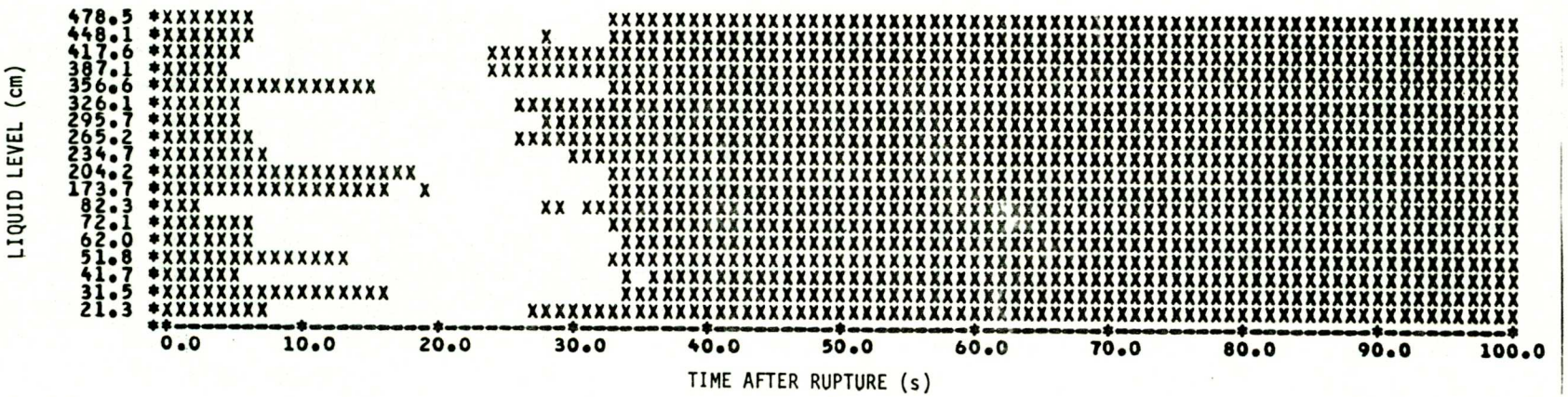

Fig. 10 Liquid level in downcomer and lower plenum under broken loop (LE-1ST).

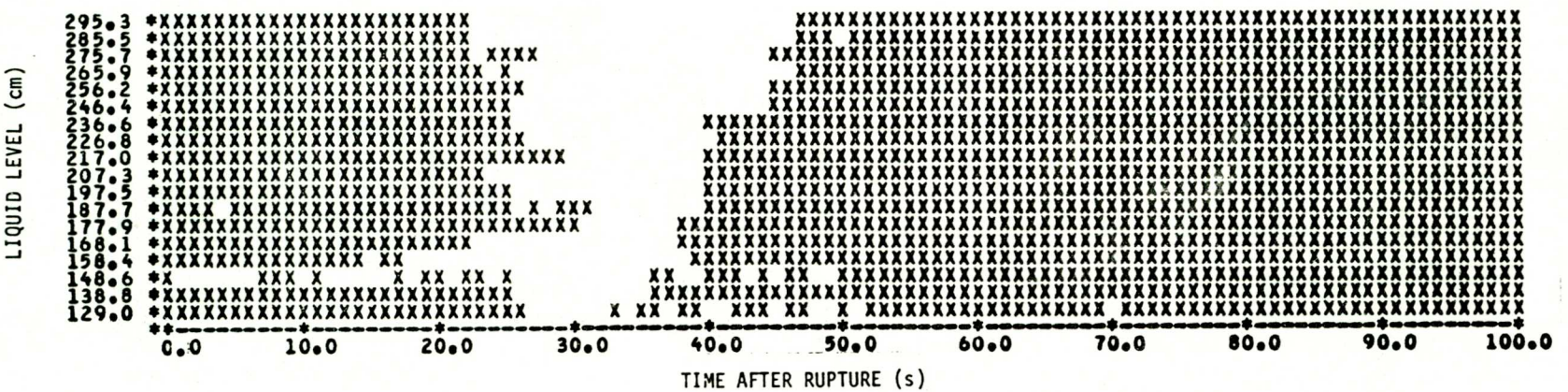

Fig. 11 Liquid level in core in Fuel Module 1 (LE-1F10).

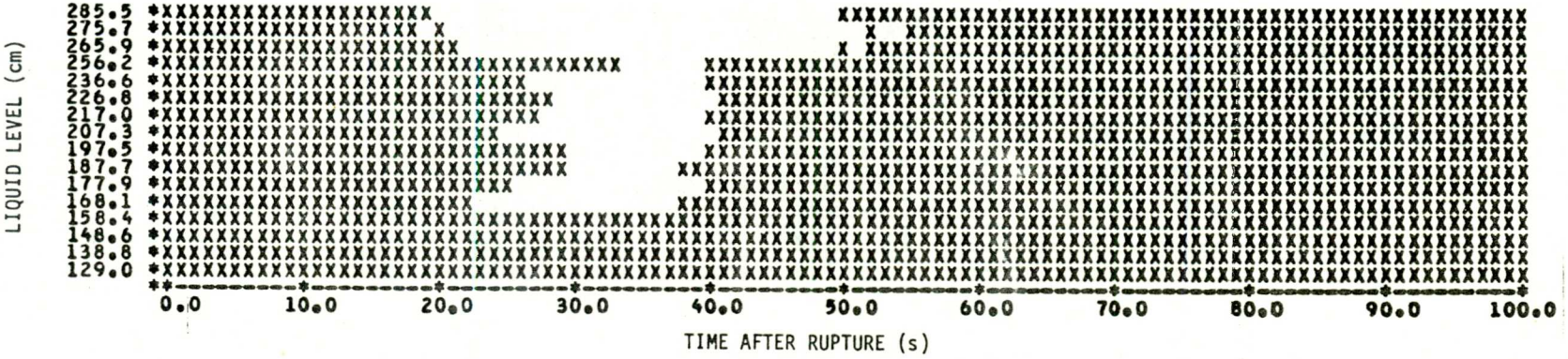

Fig. 12 Liquid level in core in Fuel Module 3 (LE-3F10).

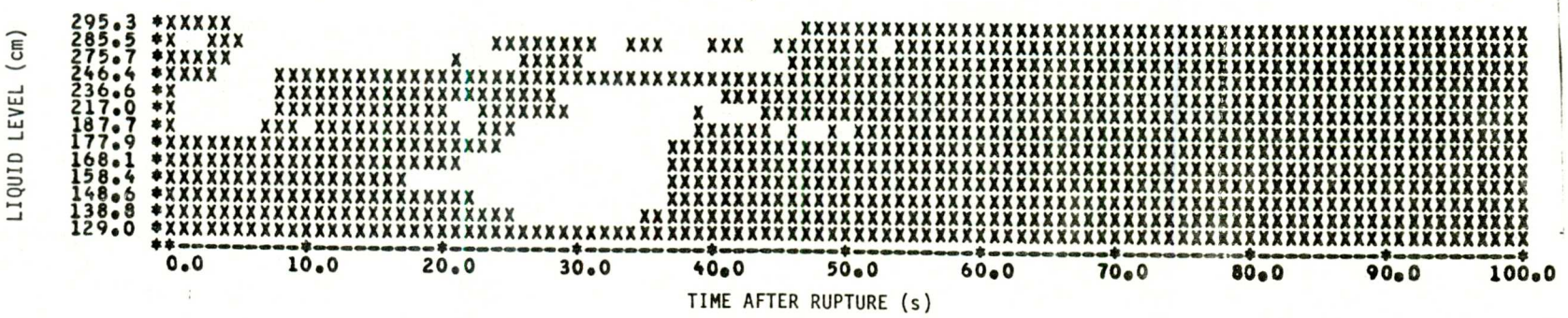

Fig. 13 Liquid level in core in Fuel Module 5 (LE-5E11).

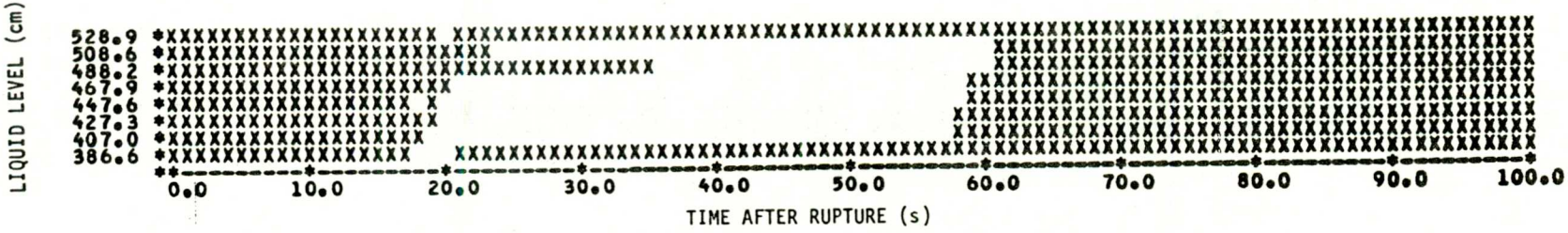

Fig. 14 Liquid level in upper plenum above Fuel Module 3 (LE-3UP).

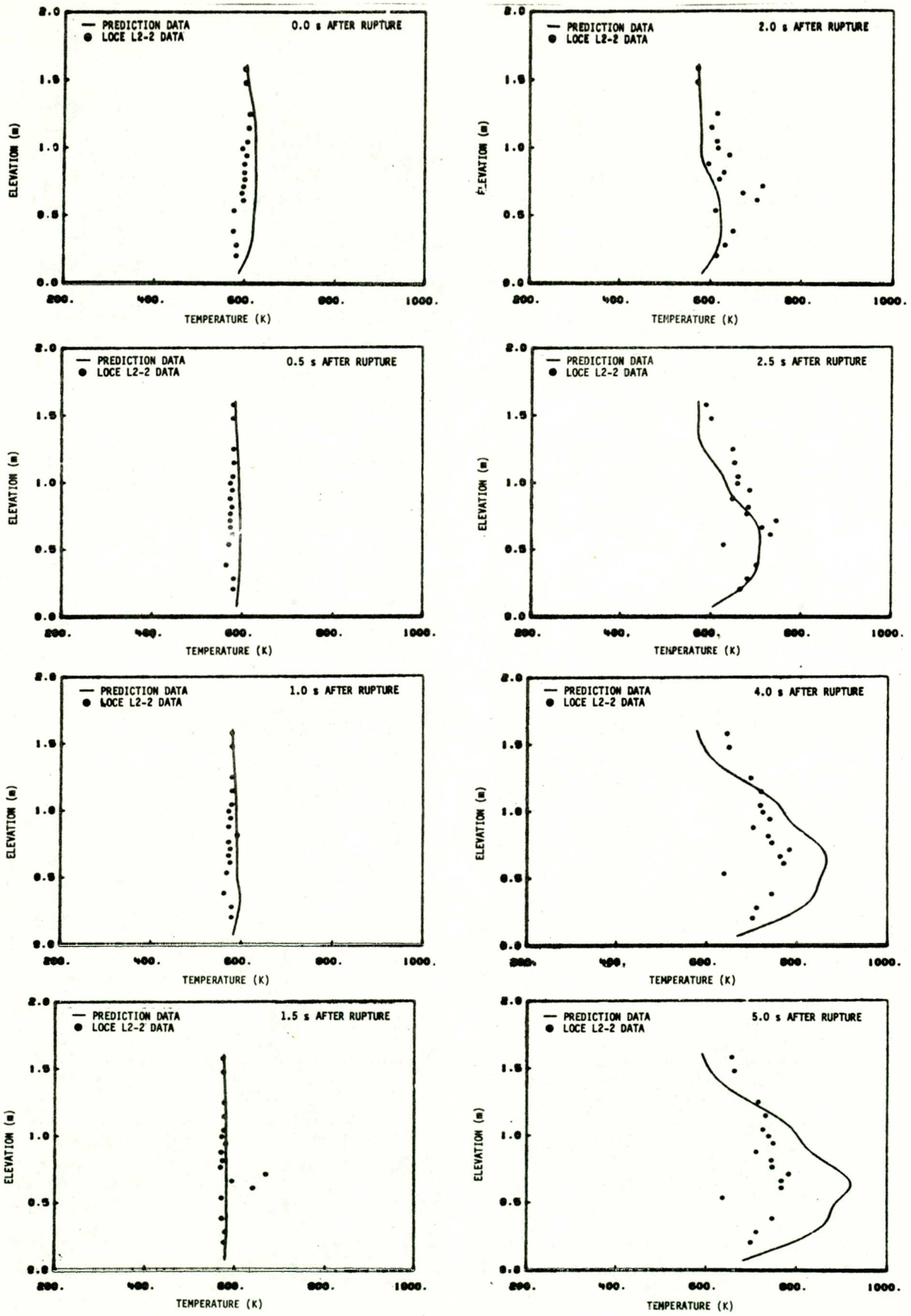

Fig. 15 Initial DNB and rise to peak cladding temperature during 0 to 5 s after rupture (center module cluster about Fuel Rod 5F8).

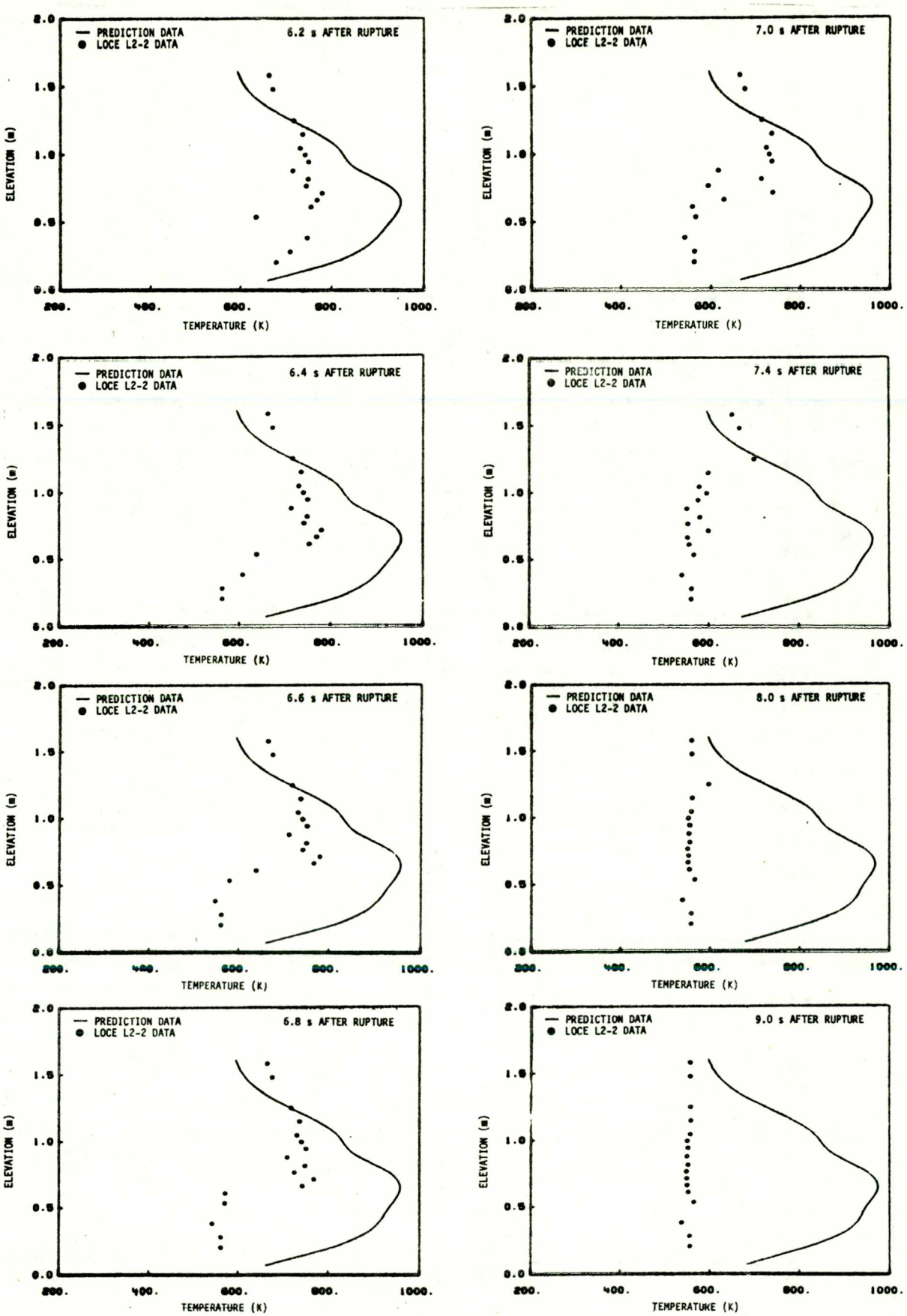

Fig. 16 Initial rewet (from bottom) during 6 to 9 s after rupture (center module cluster about Fuel Rod 5F8).

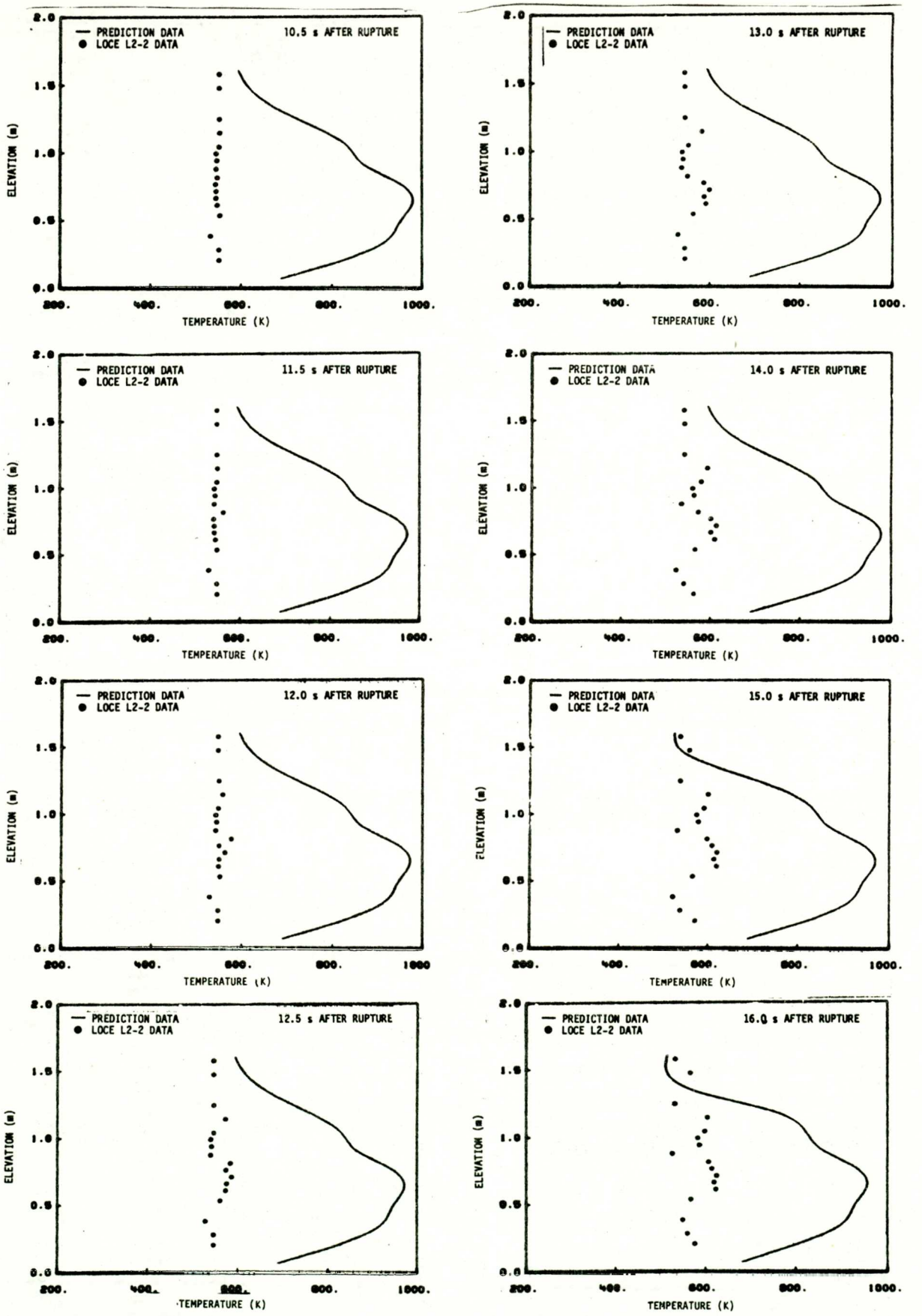

Fig. 17 First dry-out during 10.5 to 16 s after rupture (center module cluster about Fuel Rod 5F8).

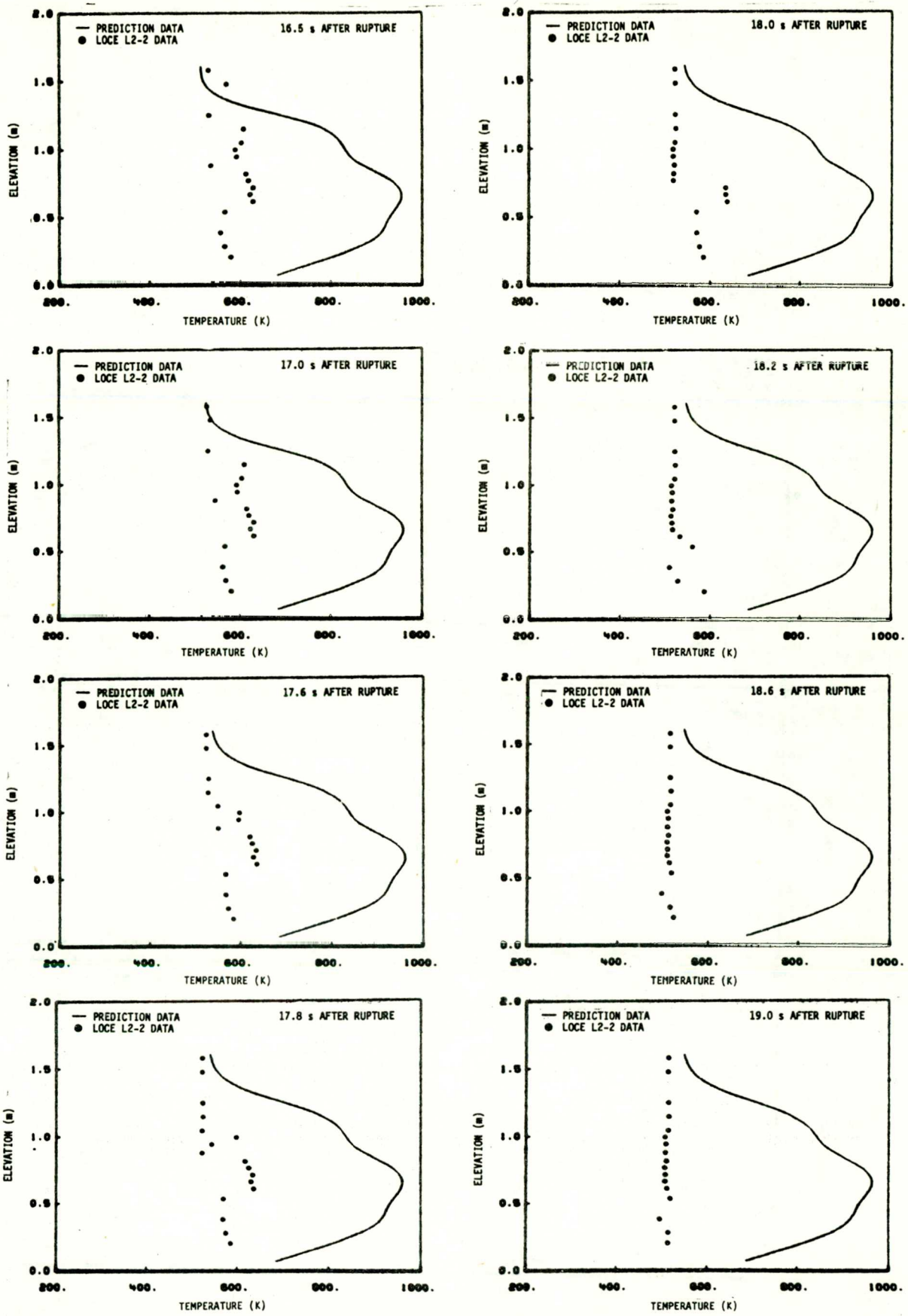

Fig. 18 Second rewet (from top) during 16.5 to 19 s after rupture (center module cluster about Fuel Rod 5F8).

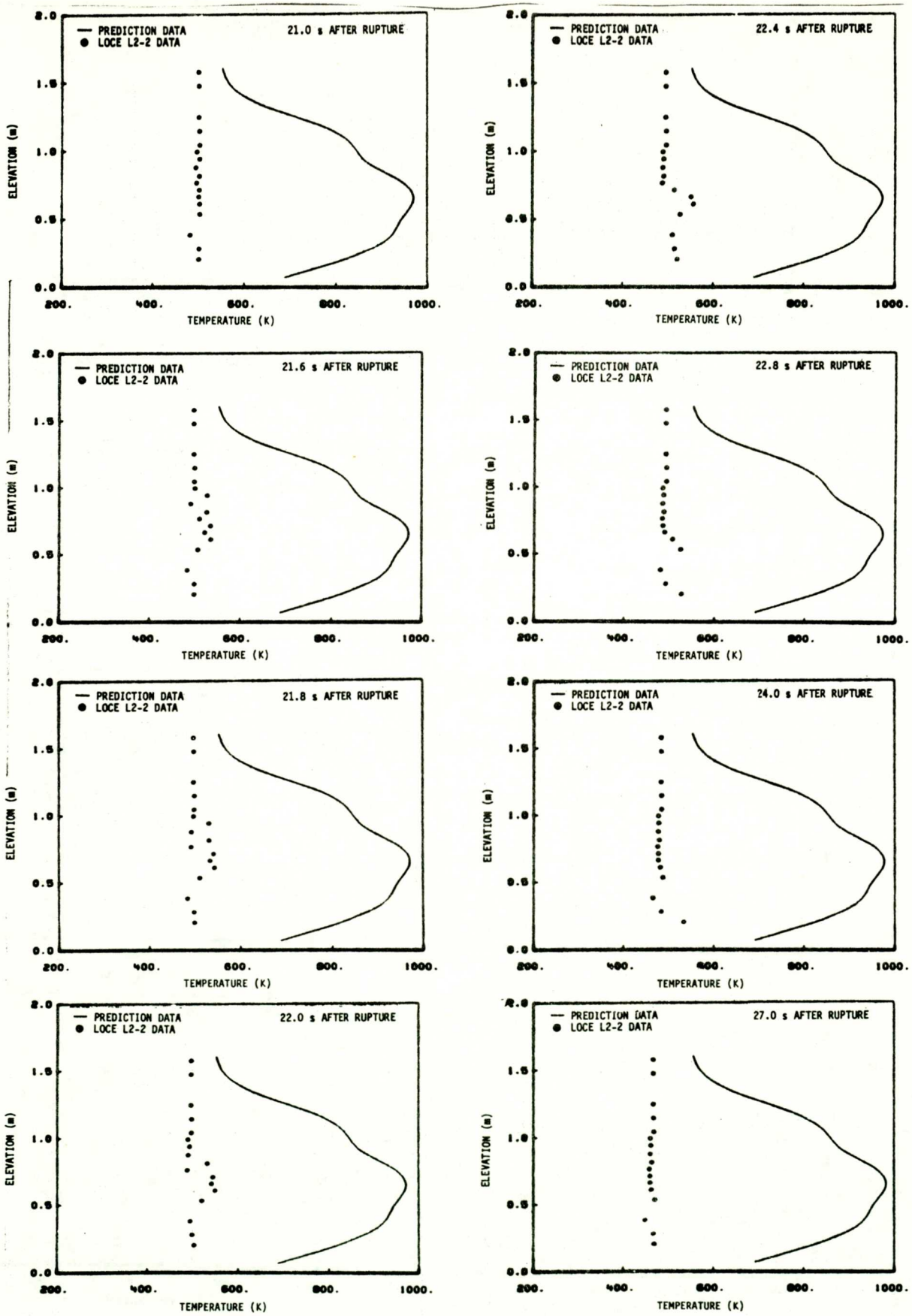

Fig. 19 Second dry-out and third rewet (from top) during 21 to 27 s after rupture (center module cluster about Fuel Rod 5F8).

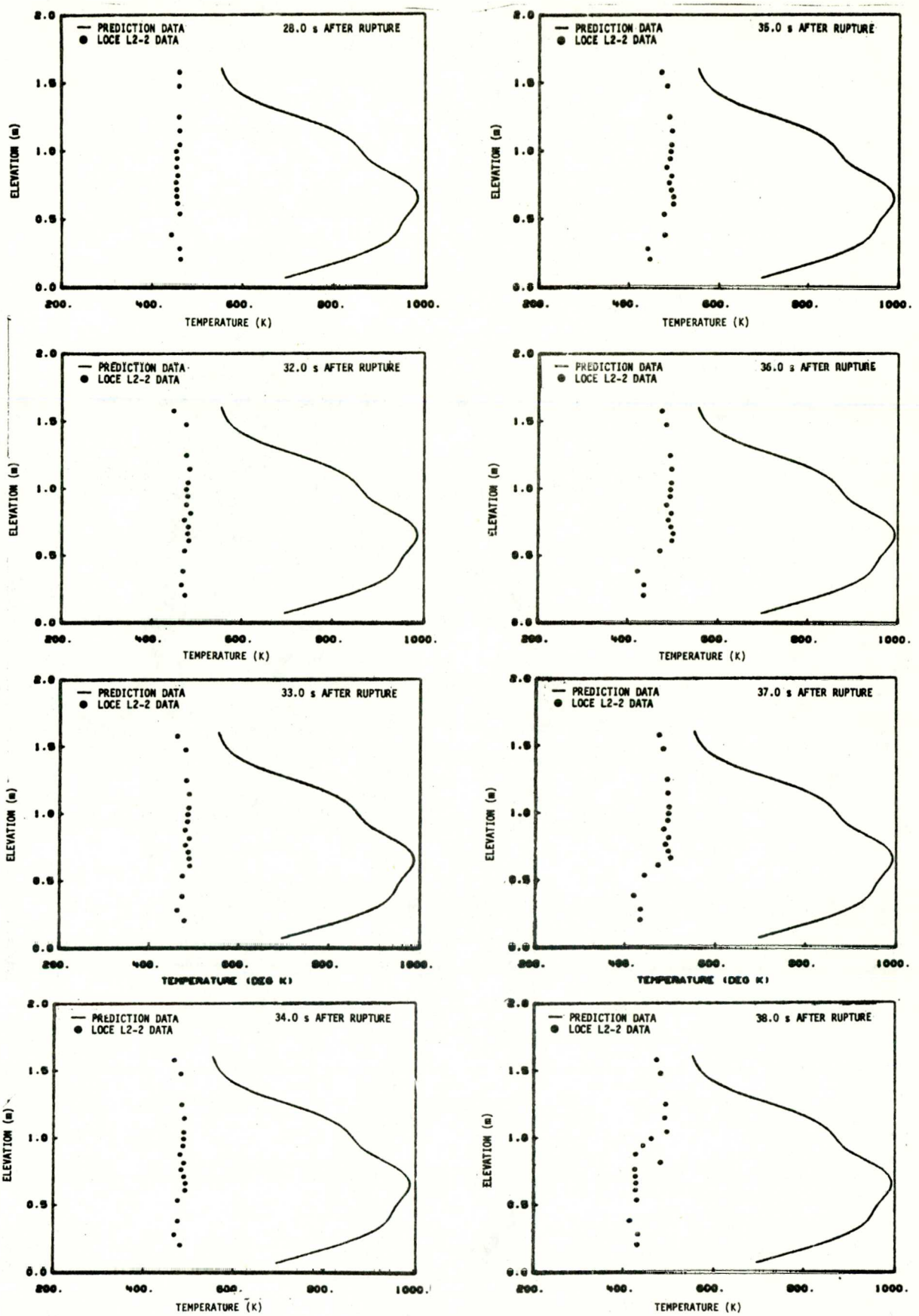

Fig. 20 Sight heatup prior to reflood quench (from bottom) during 28 to 38 s after rupture (center module cluster about Fuel Rod 5F8).

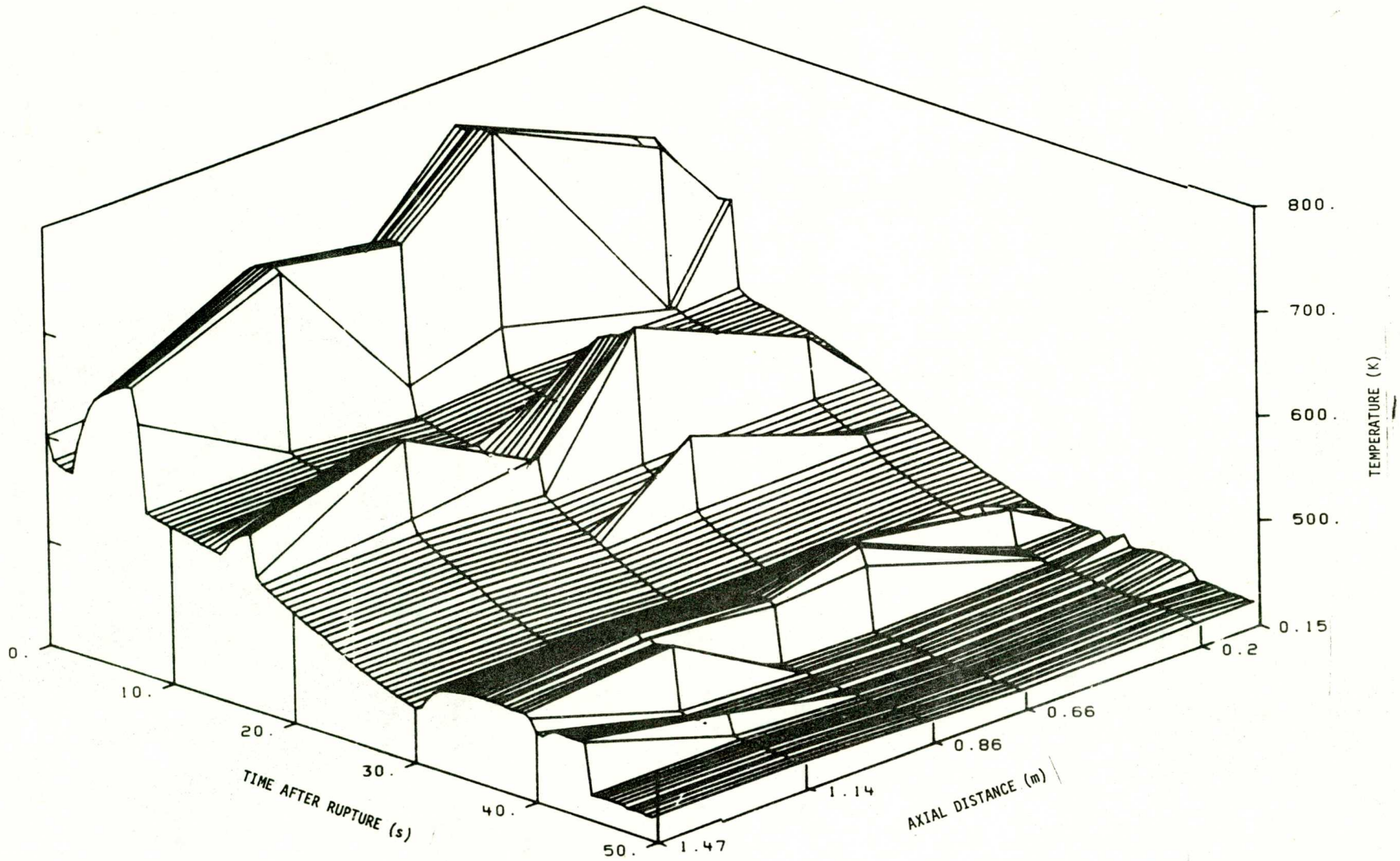

Fig. 21 Three-dimensional axial profile of cladding temperature of Fuel Module 5 (TE-5G8-58, TE-5F9-45, TE-5E8-34.5, TE-5G8-26, TE-5F9-11, and TE-5LP-2).

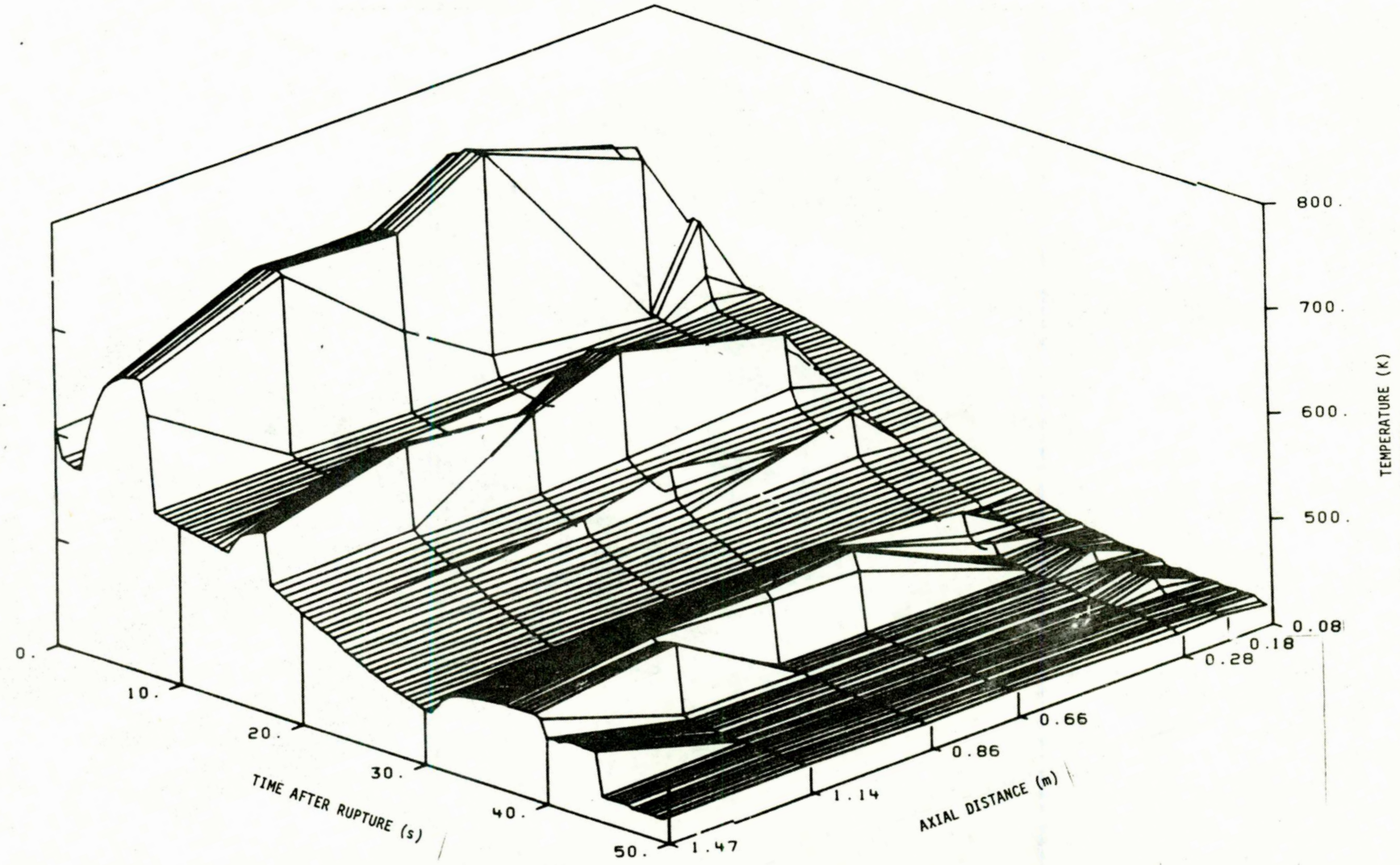

Fig. 22 Three-dimensional axial profile of cladding temperature of Fuel Module 5 (TE-5UP-7, TE-5I8-58, TE-5J7-45, TE-5K8-34.5, TE-5I8-26, TE-5J7-11, and TE-5LP-3).

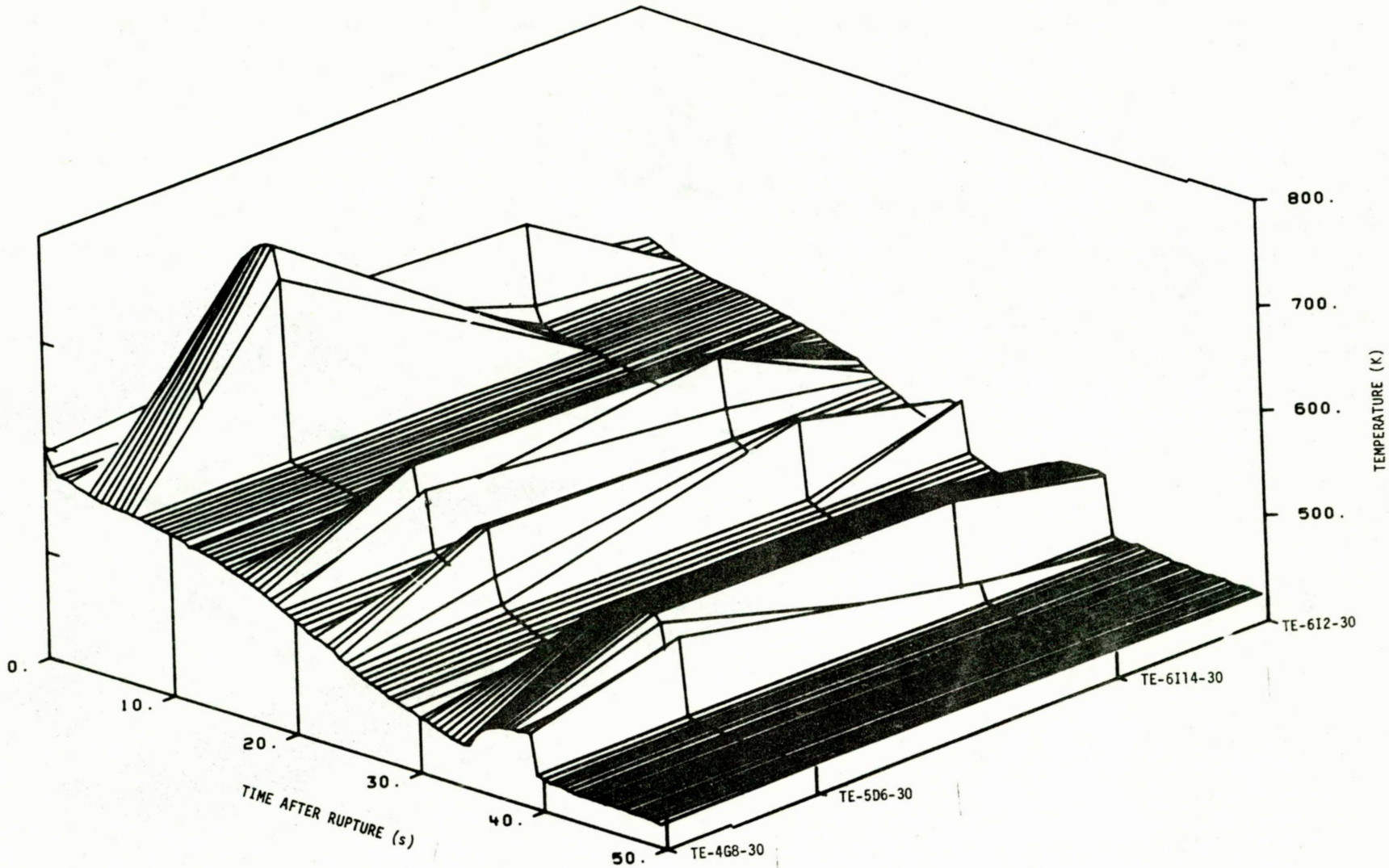

Fig. 23 Three-dimensional radial profile at 0.76-m core elevation (TE-6I2-30, TE-6I14-30, TE-5D6-30, and TE-4G8-30).

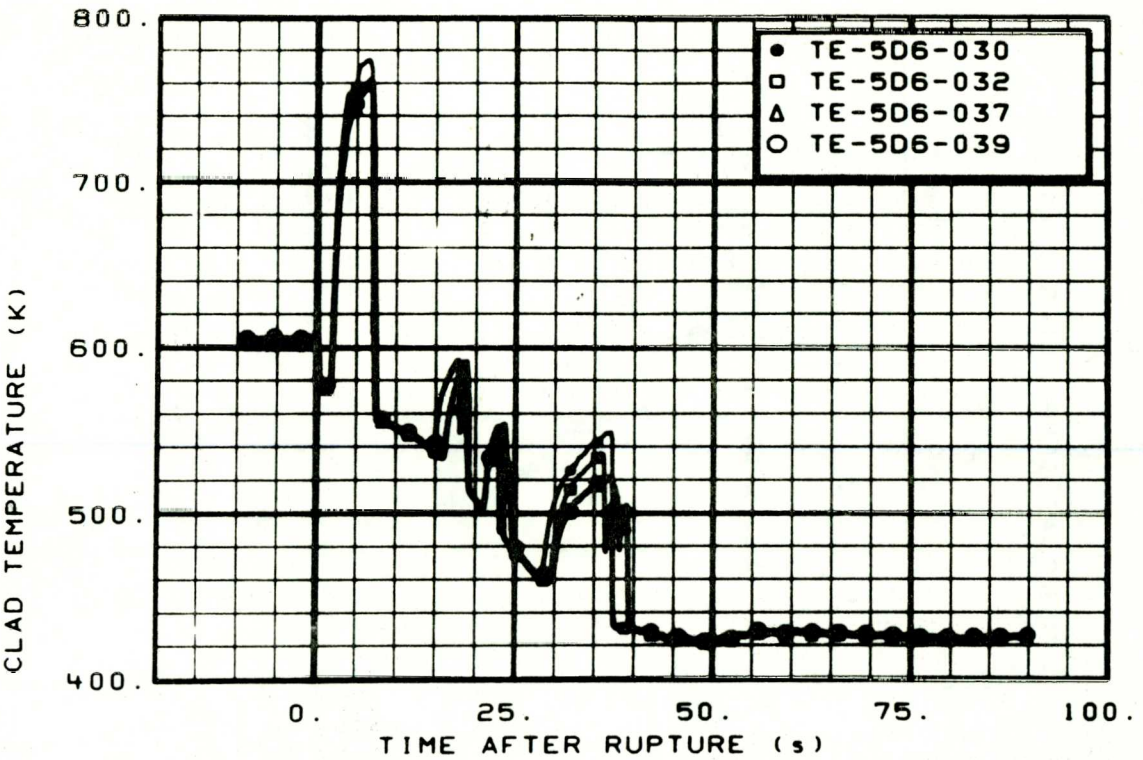

Fig. 24 Temperature of cladding of Fuel Module 5, Rod D6 (TE-5D6-30, -32, -37, and -39).

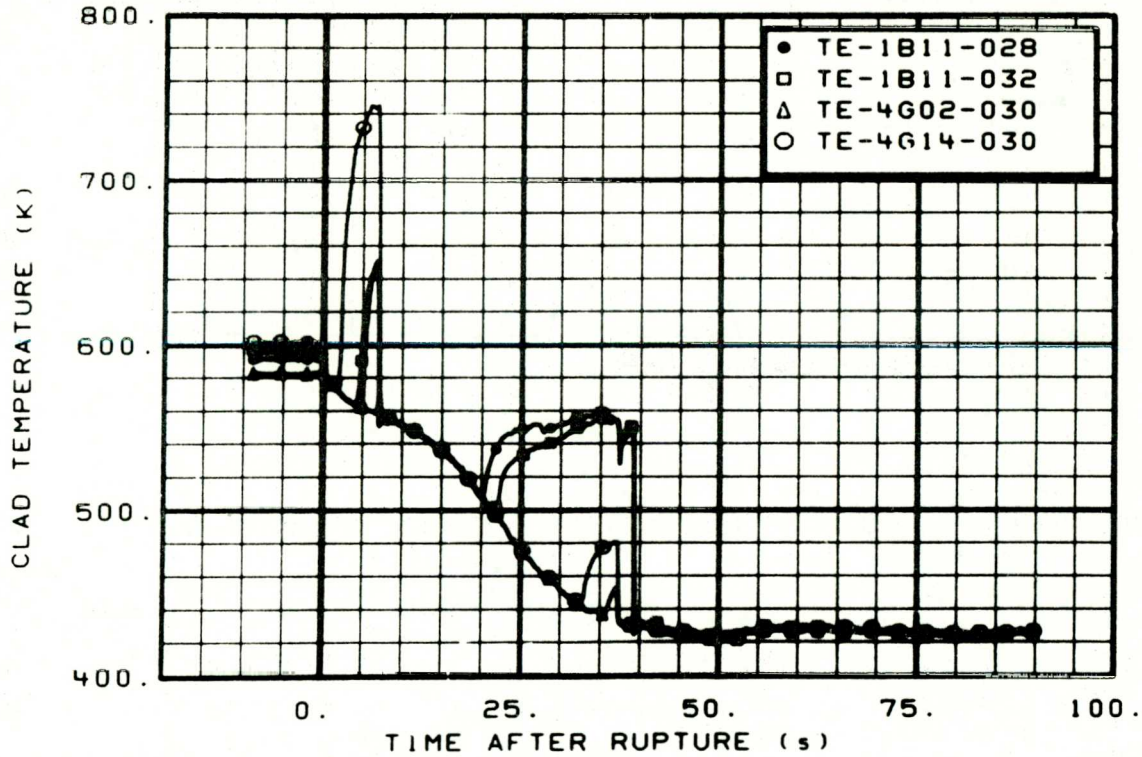

Fig. 25 Temperature of cladding of Fuel Module 1, Rod B11 and of Fuel Module 4, Rods G2 and G14 (TE-1B11-28 and -32, TE-4G02-30, and TE-4G14-30).

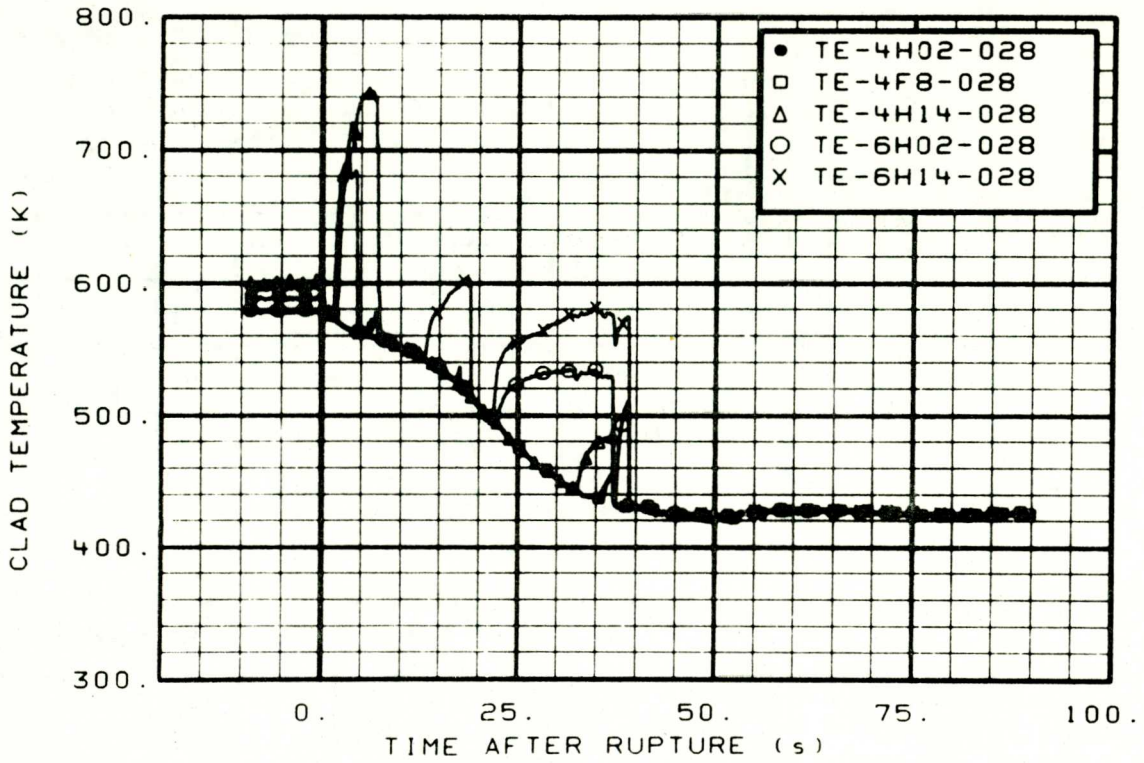

Fig. 26 Temperature of cladding of Fuel Module 4, Rods H02, H14, F8 and Fuel Module 6, Rods 6H02 and 6H14 (TE-4H02-028, TE-4F8-028, TE-4H14-28, TE-6H02-028, and TE-6H14-028).

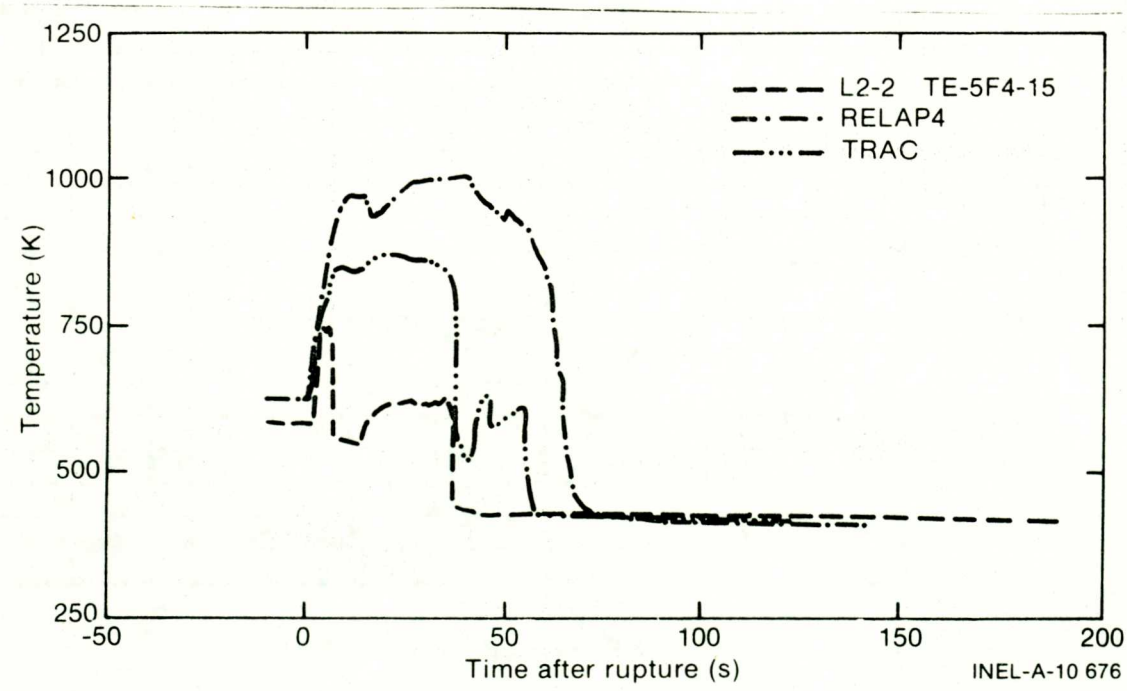

Fig. 27 Temperature of cladding of Fuel Module 5, Rod F4 for LOCE L2-2 data (TE-5F4-15), TRAC, and RELAP4 calculations.

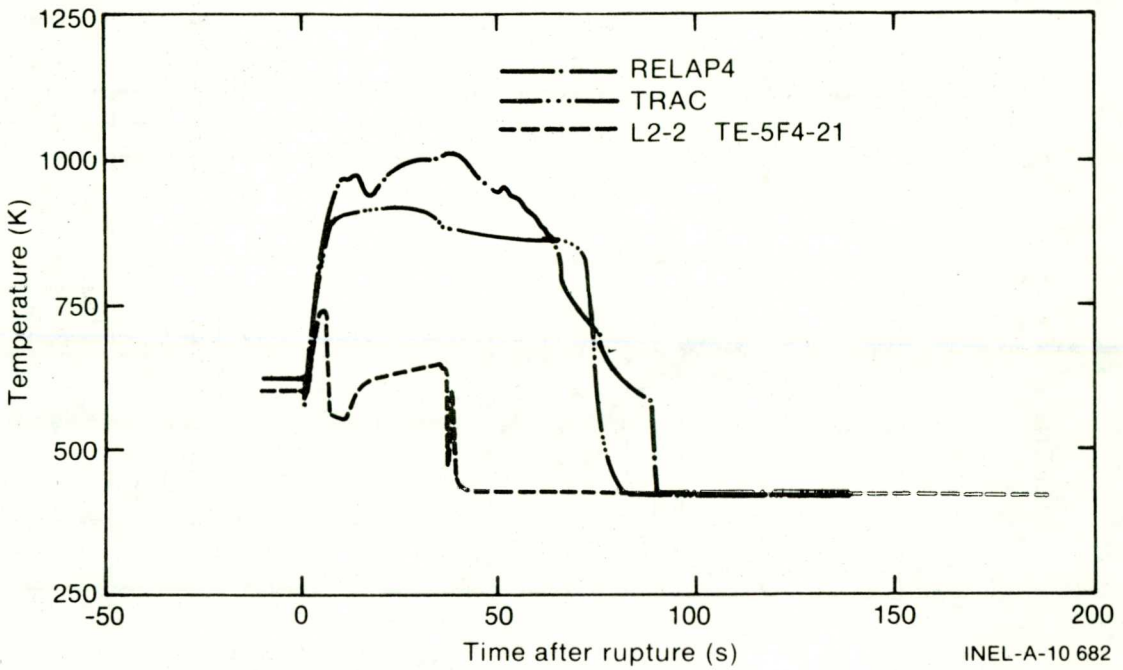

Fig. 28 Temperature of cladding of Fuel Module 5, Rod F4 for LOCE L2-2 data (TE-5F4-21), TRAC, and RELAP4 calculations.

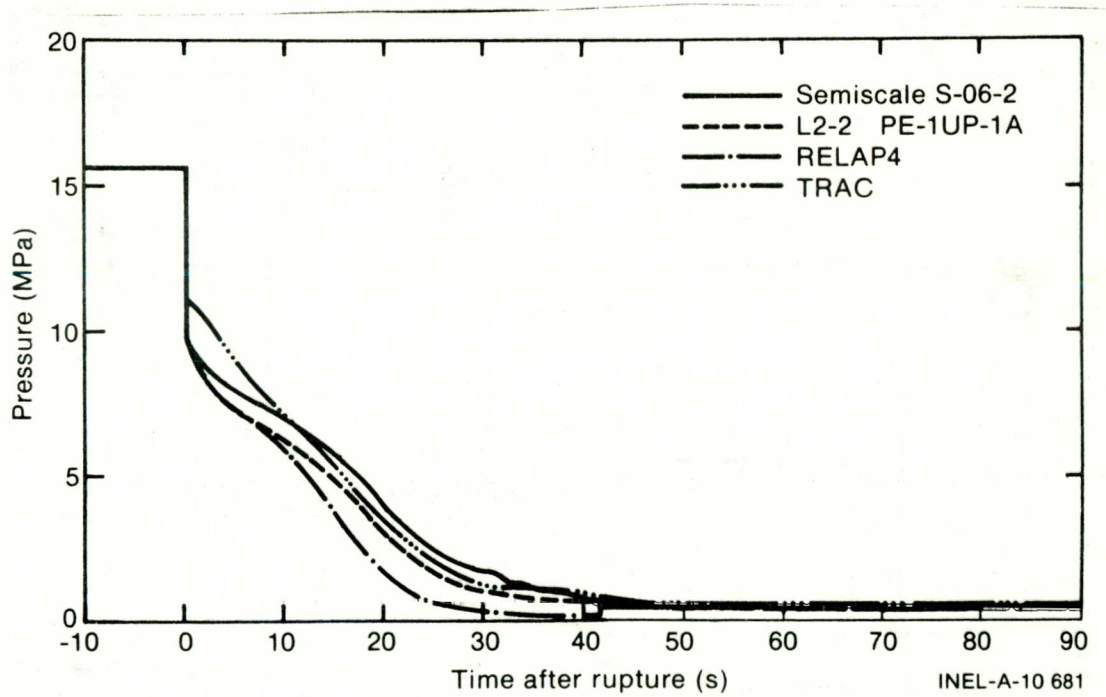

Fig. 29 Pressure in upper plenum for Semiscale Test S-06-2, LOFT LOCE L2-2 (PE-1UP-1A), RELAP4, and TRAC.

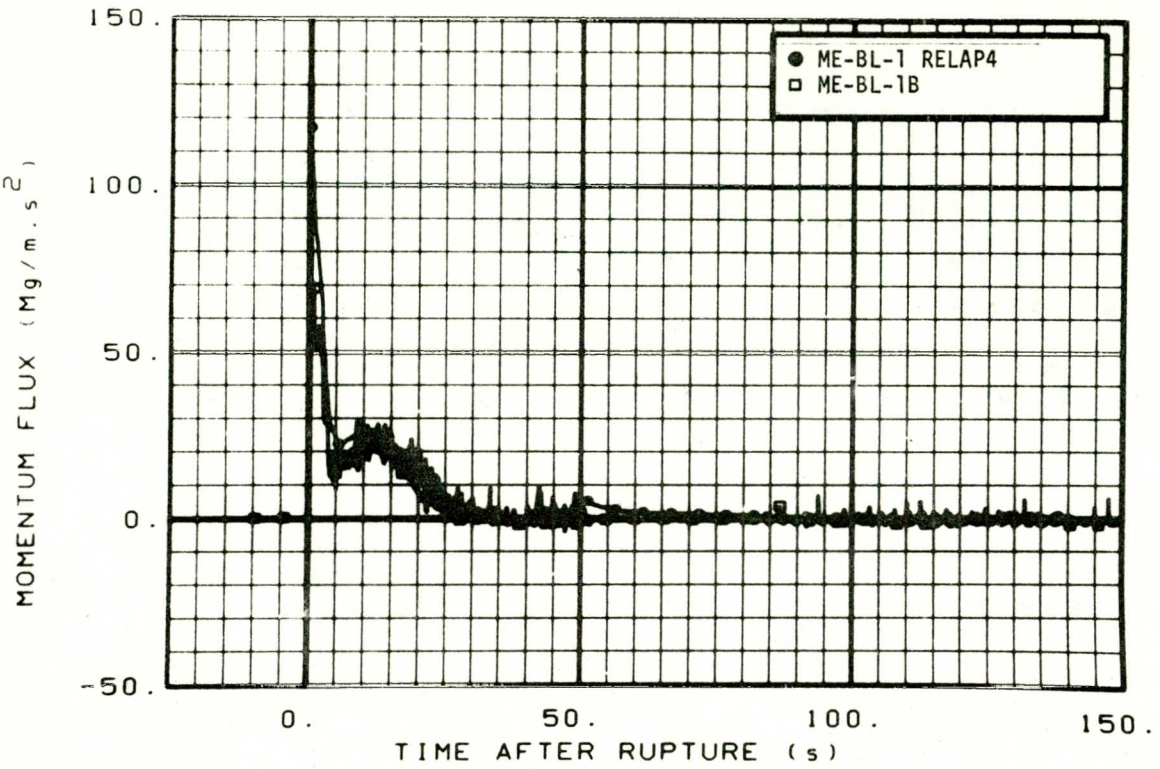

Fig. 30 Momentum flux in broken loop cold leg for RELAP4 and LOCE L2-2 data (ME-BL-1B).

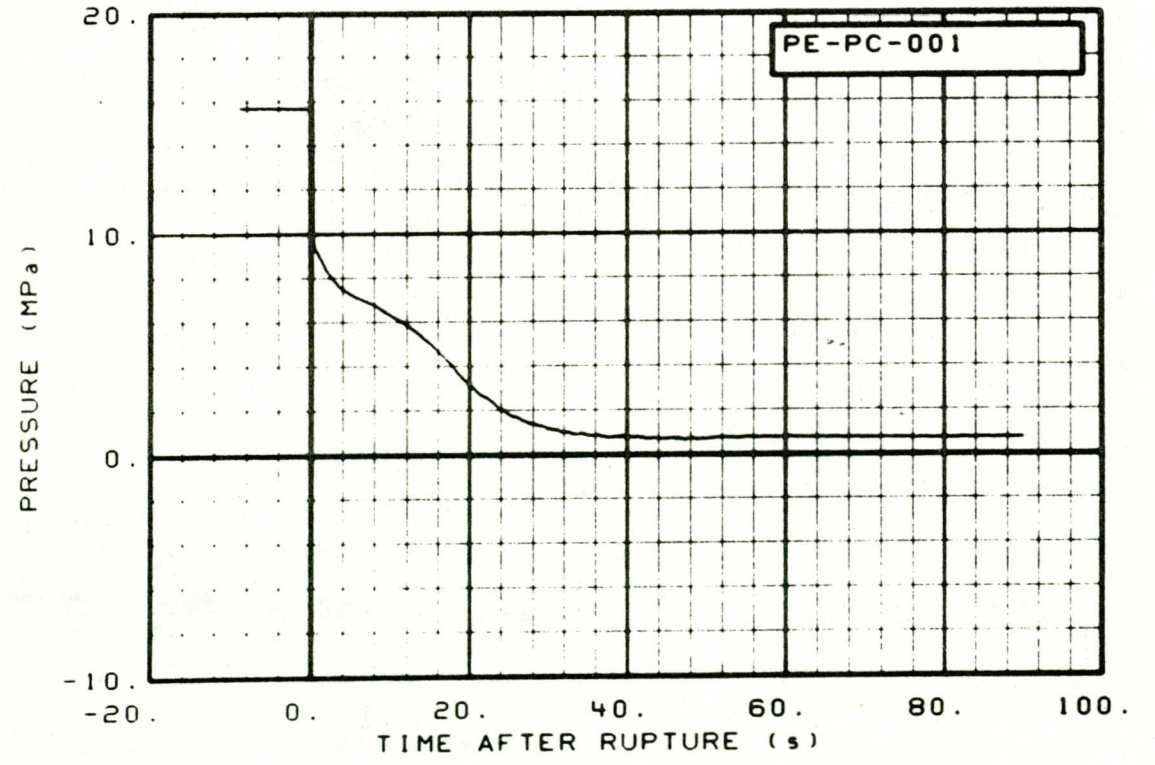

Fig. 31 Pressure in intact loop cold leg (PE-PC-1).

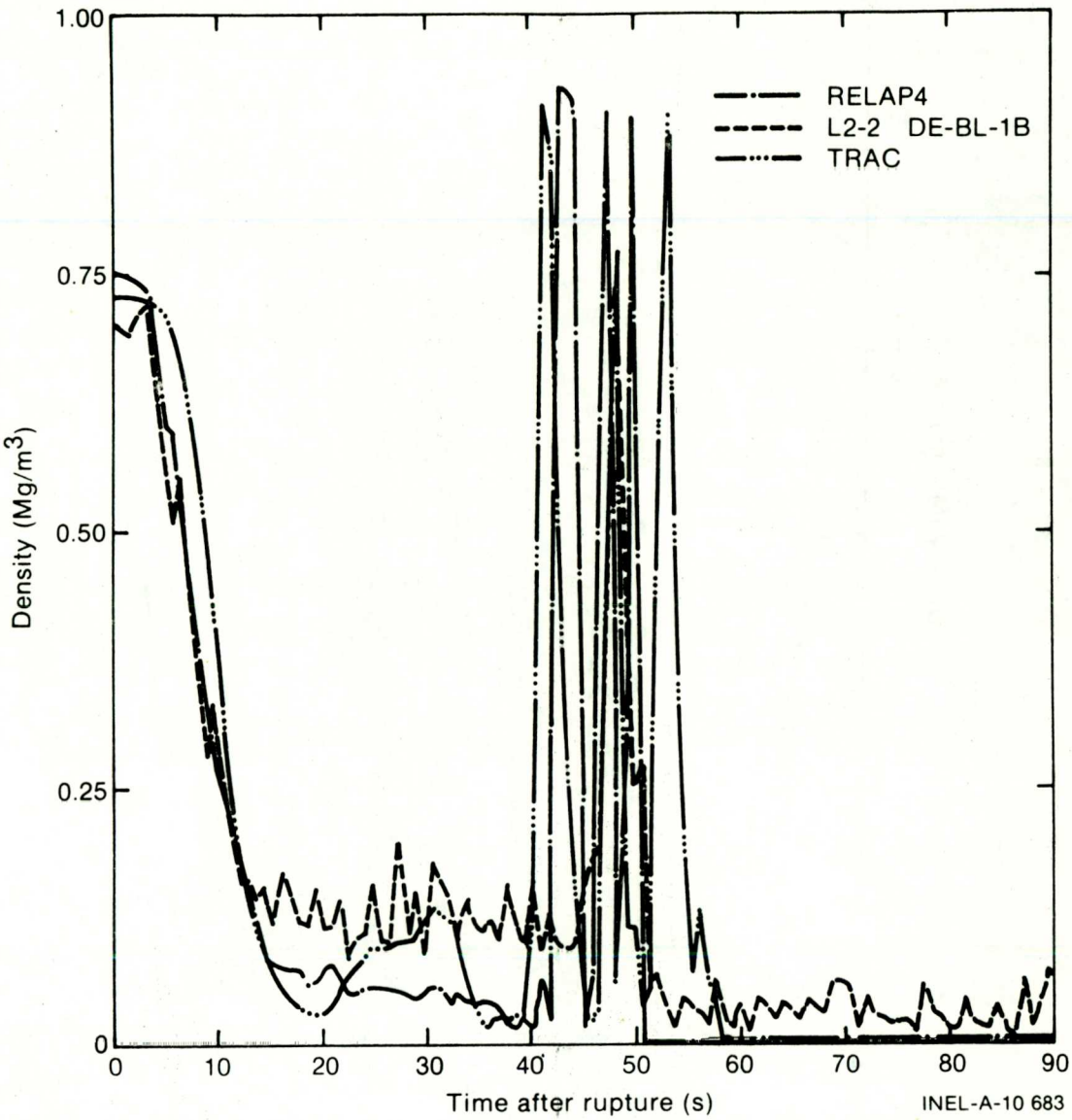

Fig. 32 Density in broken loop cold leg (DE-BL-1B).

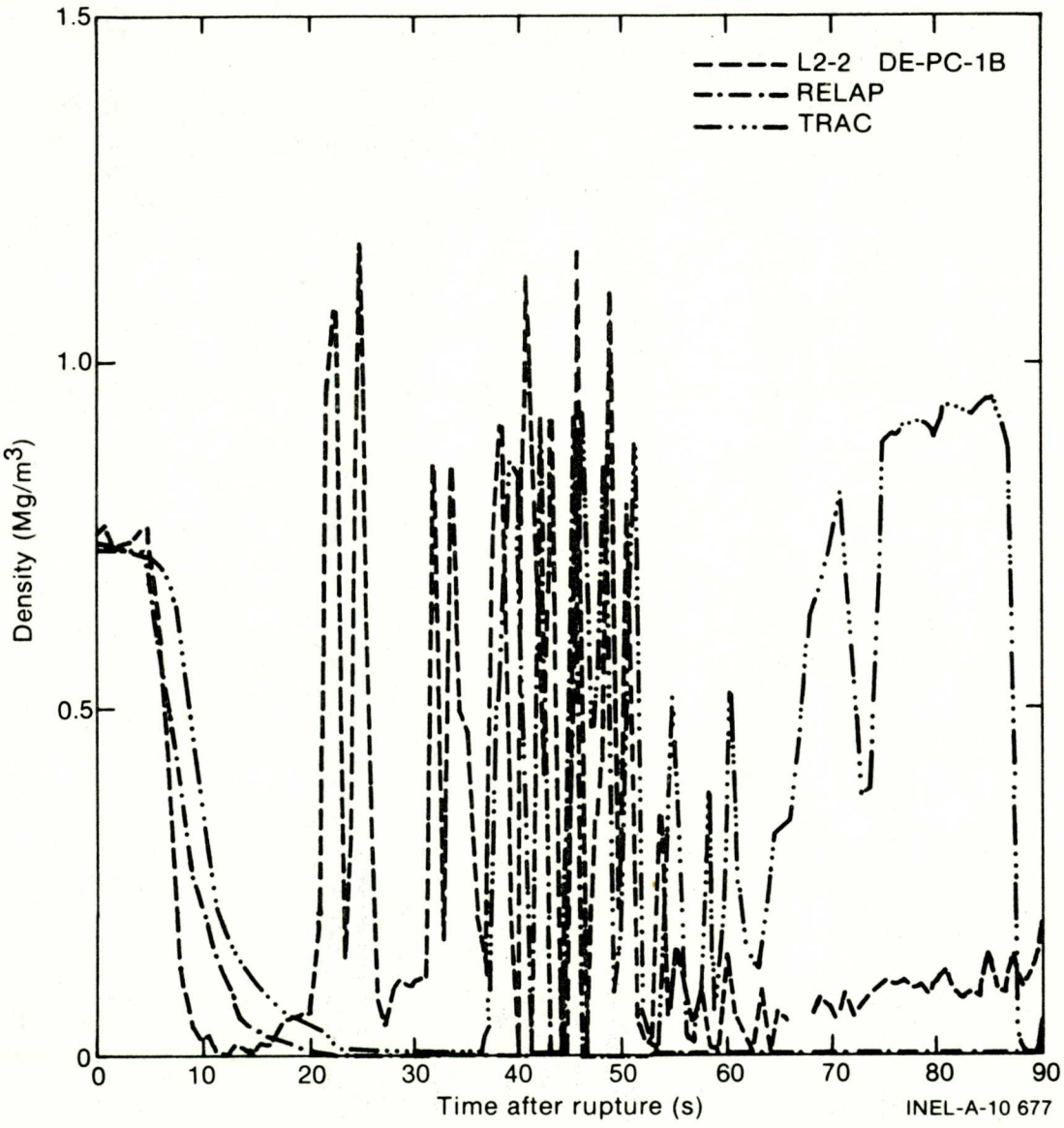

Fig. 33 Density in intact loop cold leg (DE-PC-1B).

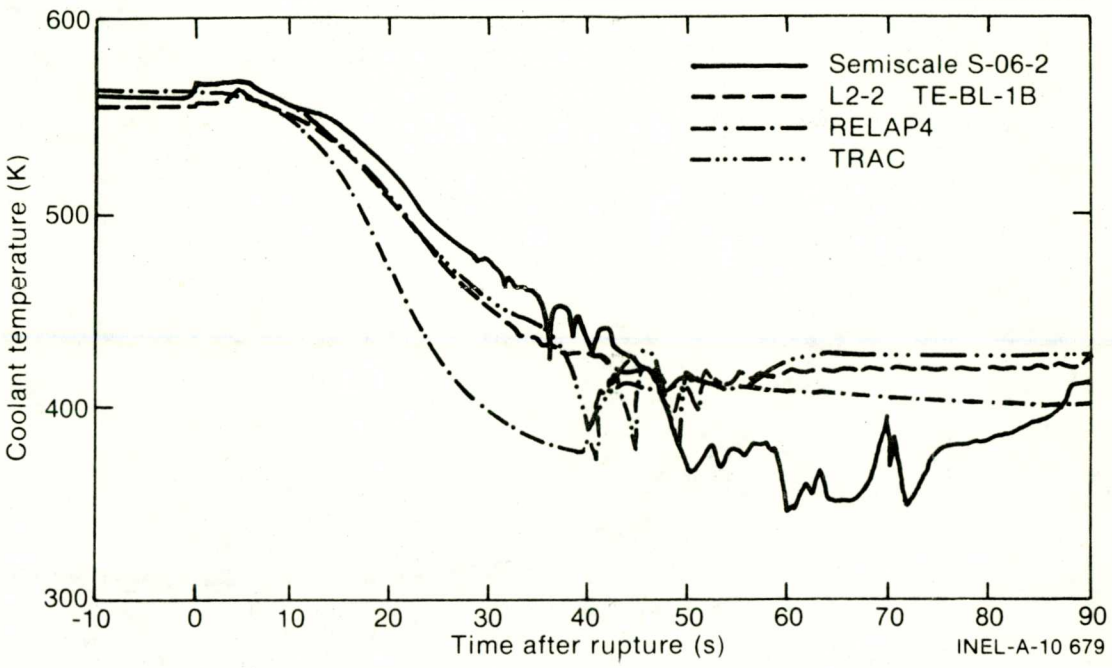

Fig. 34 Temperature in broken loop cold leg (TE-BL-1B).

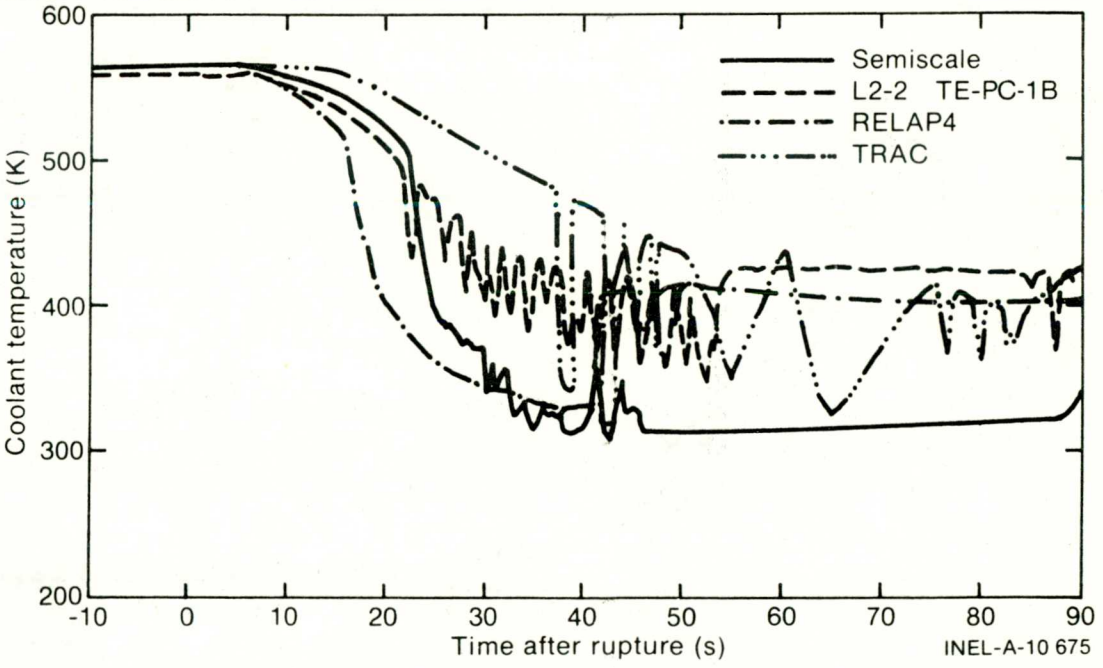

Fig. 35 Temperature in intact loop cold leg (TE-PC-1B).

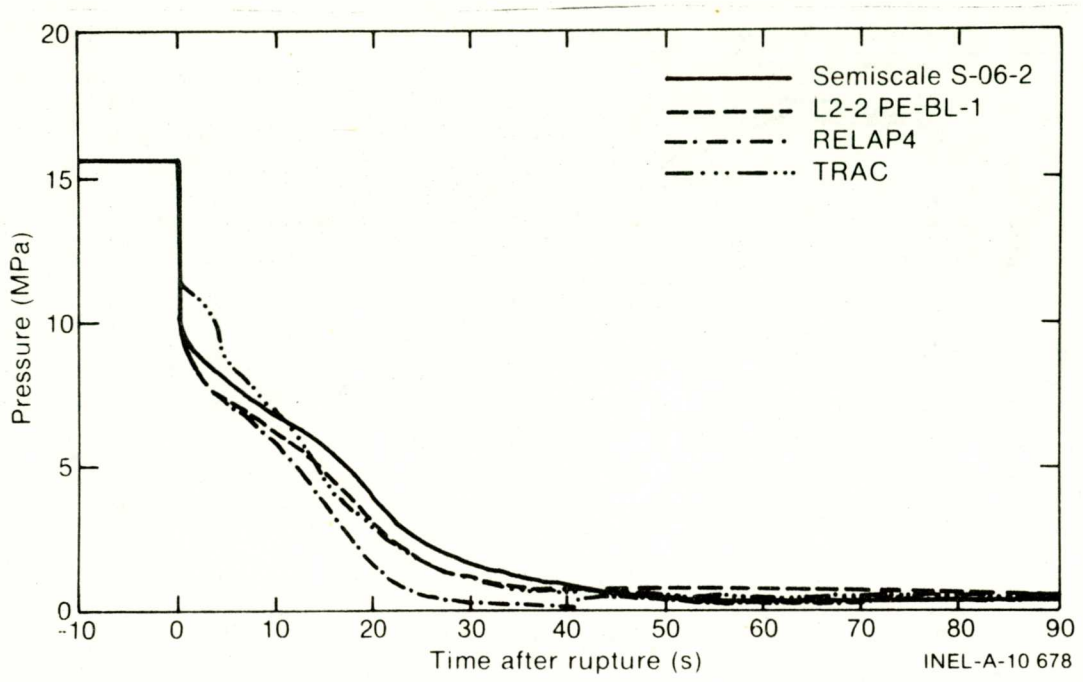

Fig. 36 Pressure in broken loop cold leg (PE-BL-1).

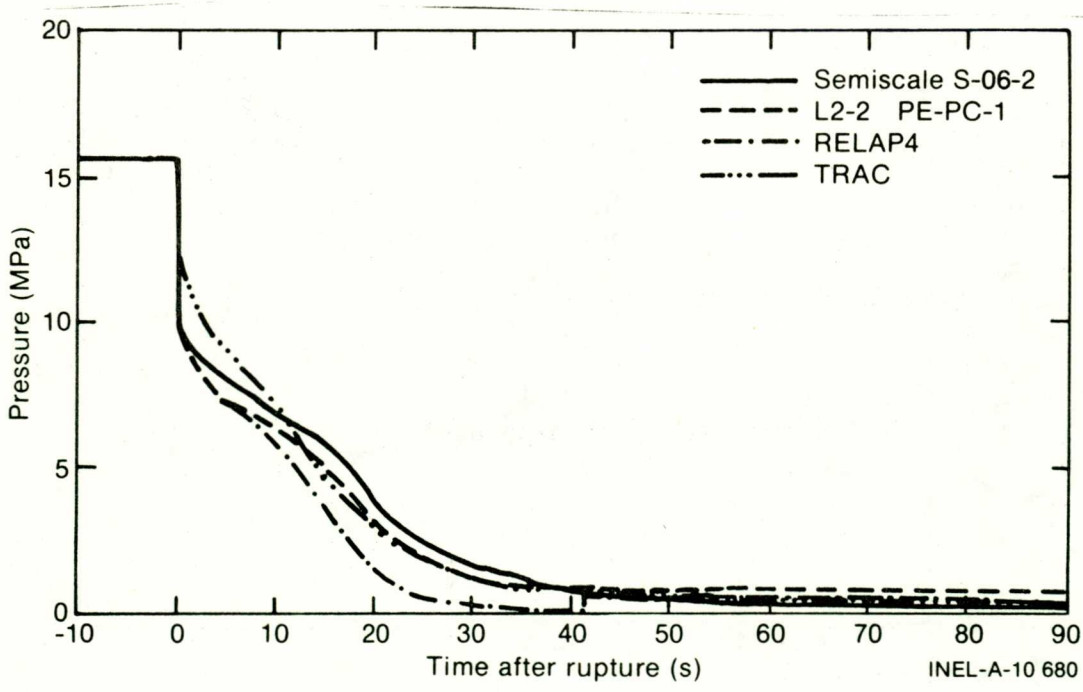

Fig. 37 Pressure in intact loop cold leg (PE-PC-1).

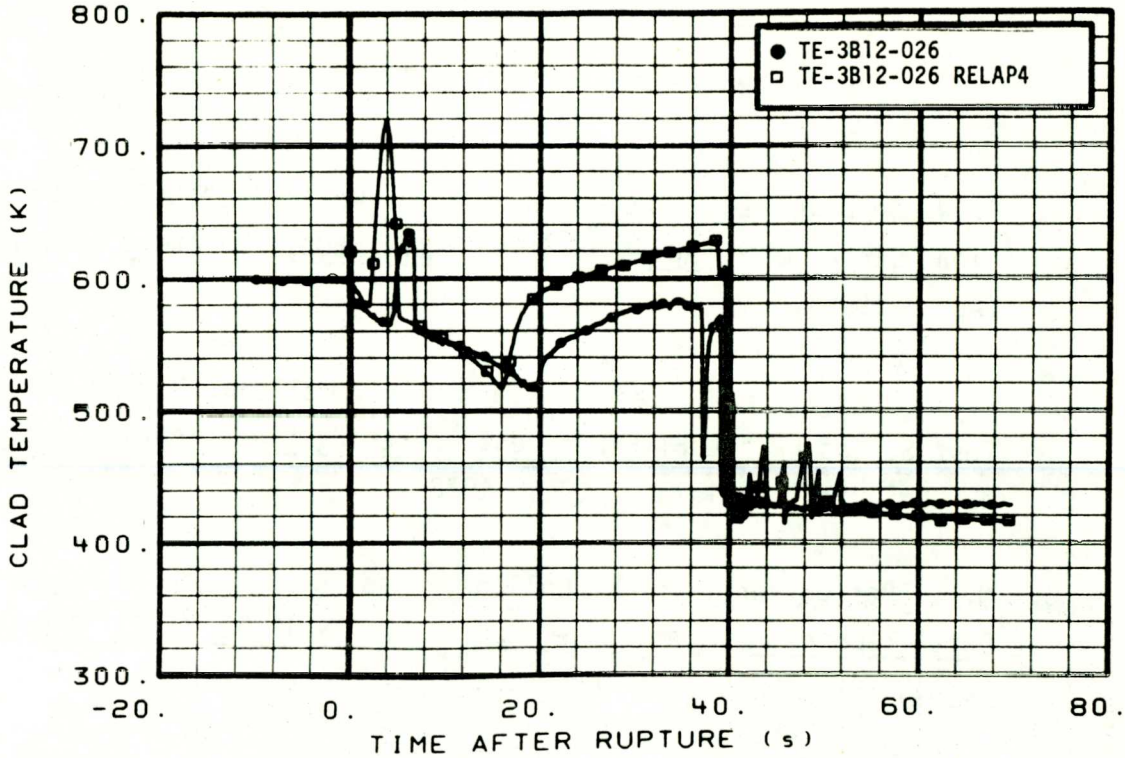

Fig. 38 Temperature of cladding on Fuel Module 3, Rod B12 for LOCE L2-2 data and RELAP4 (TE-3B12-026).

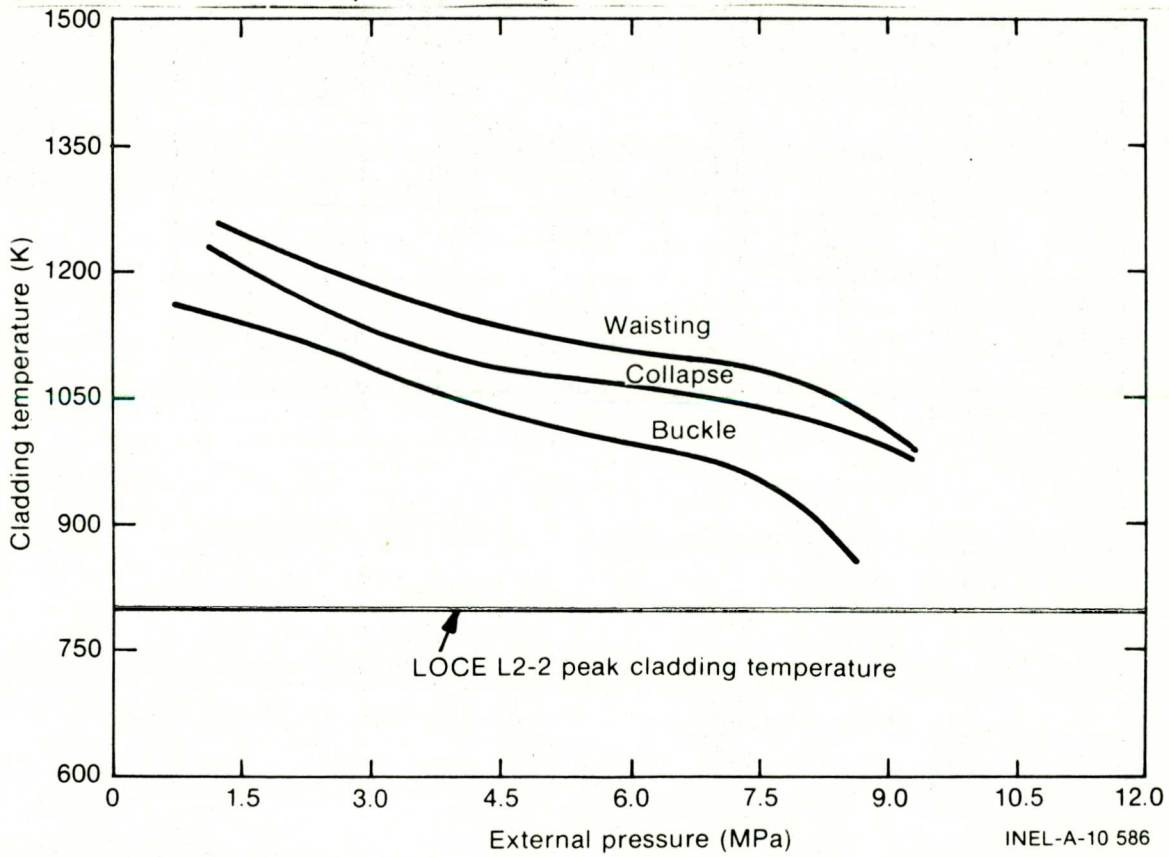

Fig. 39 Modes of cladding deformation at different pressures and temperatures maintained for 15 s.

6. REFERENCES

1. C. W. Solbrig, L. P. Leach, and H. J. Welland, "LOFT Power Ascension Series L2," Appendix B to LOFT EOS, Volume 1, Revision 1 (April 1978).

2. P. A. Harris, T. K. Samuels, and H. J. Welland, "Power Ascension Test Series L2," LOFT Experiment Operating Specification, Volume 2, NE L2 Series, Revision 2 (July 1978).

3. M. L. Patton, Jr., B. L. Collins, and K. E. Sackett, Experiment Data Report for Semiscale Mod-1 Test S-06-02 (LOFT Counterpart Test), TREE-NUREG-1122 (August 1977).

4. W. H. Grush et al, Best Estimate Experiment Predictions for LOFT Nuclear Experiments L2-2, L2-3, and L2-4, LOFT-TR-101 (November 1978).

5. EG&G Idaho, Inc., RELAP4/MOD6 -- A Computer Program for Transient Thermal-Hydraulic Analysis of Nuclear Reactors and Related Systems -- User's Manual, CDAP-TR-003 (January 1978).

6. L. J. Siefken et al, FRAP-T4 -- A Computer Code for the Transient Analysis of Oxide Fuel Rods, CDAP-TR-78-027 (July 1978).

7. Los Alamos Scientific Laboratory, TRAC-P1: An Advanced Best Estimate Computing Program for PWR LOCA Analysis, LA-NUREG/CR-0063 (June 1978).

8. K. A. Williams, TRAC Pretest Prediction of LOFT Nuclear Test L2-2, Los Alamos Scientific Laboratory Report LA-UR-78-3184 (December 1978).

9. D. L. Reeder, LOFT System and Test Description (5.5-ft Nuclear Core 1 LOCEs), NUREG/CR-0247, TREE-1208 (July 1978).

10. C. S. Olsen, Zircaloy Cladding Collapse Under Off-Normal Temperature and Pressure Conditions, TREE-NUREG-1239 (April 1978).